Detection of Multivariate Cyclostationarity

David Ramírez, *Member, IEEE*, Peter J. Schreier, *Senior Member, IEEE*, Javier Vía, *Senior Member, IEEE*, Ignacio Santamaría, *Senior Member, IEEE*, and Louis L. Scharf, *Life Fellow, IEEE*

***Abstract*—This paper derives an asymptotic generalized likelihood ratio test (GLRT) and an asymptotic locally most powerful invariant test (LMPIT) for two hypothesis testing problems: 1) Is a vector-valued random process cyclostationary (CS) or is it wide-sense stationary (WSS)? 2) Is a vector-valued random process CS or is it nonstationary? Our approach uses the relationship between a scalar-valued CS time series and a vector-valued WSS time series for which the knowledge of the cycle period is required. This relationship allows us to formulate the problem as a test for the covariance structure of the observations. The covariance matrix of the observations has a block-Toeplitz structure for CS and WSS processes. By considering the asymptotic case where the covariance matrix becomes block-circulant we are able to derive its maximum likelihood (ML) estimate and thus an asymptotic GLRT. Moreover, using Wijsman's theorem, we also obtain an asymptotic LMPIT. These detectors may be expressed in terms of the Loève spectrum, the cyclic spectrum, and the power spectral density, establishing how to fuse the information in these spectra for an asymptotic GLRT and LMPIT. This goes beyond the state-of-the-art, where it is common practice to build detectors of cyclostationarity from *ad-hoc* functions of these spectra.**

***Index Terms*—Cyclostationarity, generalized likelihood ratio test (GLRT), locally most powerful invariant test (LMPIT), Toeplitz matrix, Wijsman's theorem.**

I. Introduction

A zero-mean, discrete-time, complex-valued random process $u[n]$ is said to be (second-order) cyclostationary (CS) if its covariance function is periodic with period P [1], [2]:

$$r_{uu}[n,m] = E[u[n]u^*[n-m]] = r_{uu}[n+P,m].$$

Manuscript received February 13, 2015; revised June 09, 2015; accepted June 11, 2015. Date of publication June 25, 2015; date of current version September 09, 2015. The associate editor coordinating the review of this manuscript and approving it for publication was Prof. Joseph Tabrikian. The work of P. Schreier was supported by the Alfried Krupp von Bohlen und Halbach Foundation, under its program "Return of German scientists from abroad". The work of I. Santamaría and J. Vía was supported by the Spanish Government, Ministerio de Ciencia e Innovación (MICINN), under project RACHEL (TEC2013-47141-C4-3-R). The work of I. Santamaría was also supported by grant PRX14-00128. The work of L. Scharf was supported by the Airforce Office of Scientific Research under contract FA9550-10-1-0241.

D. Ramírez and P. J. Schreier are with the Department of Electrical Engineering and Information Technology, University of Paderborn, 33098 Paderborn, Germany (e-mail: david.ramirez@sst.upb.de; peter.schreier@sst.upb.de).

J. Vía and I. Santamaría are with the Department of Communications Engineering, University of Cantabria, 39005 Santander, Spain (e-mail: jvia@gtas.dicom.unican.es; nacho@gtas.dicom.unican.es).

L. L. Scharf is with the Departments of Mathematics and Statistics, Colorado State University, Ft. Collins, CO 80523 USA (e-mail: scharf@engr.colostate.edu).

Color versions of one or more of the figures in this paper are available online at http://ieeexplore.ieee.org.

Digital Object Identifier 10.1109/TSP.2015.2450201

The period P is a natural number greater than 1 because $P = 1$ corresponds to a wide-sense stationary (WSS) process. CS signals model phenomena generated by periodic effects in communications [3] (where the periodicity is induced by modulation, sampling, and multiplexing operations), meteorology and climatology [4]–[6], oceanography [7]–[9], astronomy [10], and economics [11]–[13]. This plethora of applications has created significant interest in the analysis of CS signals as evidenced by the published literature [14], [15].

The detection of cyclostationarity is particularly important, for two main reasons. Firstly, if a signal is CS then this fact can usually be exploited in applications to improve estimation performance. However, treating a signal as CS—when in fact it is not—generally leads to very poor performance. Secondly, the presence or absence of CS signals can be used to trigger other actions. This is the case in cognitive radio (CR), which is a new communications technology that has the potential to boost spectrum usage [16]–[18]. The main idea behind CR is the opportunistic access of some users (so-called "cognitive" or "secondary" users) to a given frequency band when the rightful owner of the band (the primary user) is not transmitting. Spectrum sensing (the detection of vacant channels) is therefore a key ingredient to CR [19]. One of the most important properties that can be exploited to detect primary users is the cyclostationarity of communications signals, but other properties, such as temporally and/or spatially uncorrelated noise, can be also utilized. For these reasons, detection of cyclostationarity has received much attention in the past [11], [20]–[23] and is now receiving a lot of renewed attention in the context of CR [24]–[31].

Detectors of cyclostationarity can roughly be classified into the following three categories:

1) *Techniques based on the Loève (or dual-frequency) spectrum*. For a harmonizable process, the Loève spectrum [32] is defined as the 2D-Fourier transform of the correlation function $r_{uu}[n,m]$. The support of the Loève spectrum of a CS process is on lines parallel to the stationary manifold [33], whereas for WSS processes the support is only one line, the stationary manifold. Several detectors [11], [20], [21] have been proposed that exploit this by comparing the values of the Loève spectrum along the lines that correspond to the CS components to the values along the line that corresponds to the WSS component. The critical question is what function to use for this comparison. The early works [11], [20], [21] use ad-hoc approaches, which are not grounded in established statistical principles. We will see later that our approach can indeed be interpreted as comparing the strengths of the CS and WSS components in the Loève spectrum, but in a statistically sound fashion.

2) *Techniques based on testing for nonzero cyclic covariance function or cyclic spectrum*. There are several works that test whether or not the estimated cyclic covariance function or cyclic spectrum are zero [22], [28], [34], [35]. This, however, raises the questions: What cycle frequencies (which harmonics) and which lags of the covariance function (or global frequencies in the cyclic spectrum) must be selected and how should they be combined? Since our detectors admit an interpretation in terms of the cyclic spectrum they show how to merge the information at each cycle frequency and global frequency.
3) *Techniques based on testing for correlation between the process and a frequency-shifted version thereof*. It was proven in [36] that there exists correlation between the CS process $u[n]$ and $v[n] = u[n]e^{-j2\pi\alpha n}$, which is $u[n]$ shifted by the cycle frequency α. This idea was first used in [37] to estimate the number of CS signals impinging on an antenna array, by applying canonical correlation analysis to the signals and their frequency-shifted versions. This has also been done in the context of CR to detect the presence of primary users [31]. These two papers test the correlation in the temporal domain, although it is also possible to do so in the frequency domain [23], where the frequency coherence between $u[n]$ and $v[n]$ is used as the detector statistic. However, these detectors only consider one lag or frequency and one cycle frequency, and it is not clear how to select these without knowledge of the true cyclic correlation. If we were to consider multiple lags, it is not apparent how we would optimally fuse the information at different lags or frequencies and cycle frequencies.

Most of the approaches in the literature are for scalar time series and relatively few works have considered vector-valued time series [24]–[26], [28], [31], even though some of the scalar detectors could easily be extended to multivariate time series. All the detectors cited here consider testing cyclostationarity vs. wide-sense stationarity. We are not aware of any detectors that test cyclostationarity vs. nonstationarity.

As we have already mentioned, most detectors of cyclostationarity are ad-hoc detectors, which are not derived from accepted statistical principles, such as the generalized likelihood ratio test (GLRT), the uniformly most powerful invariant test (UMPIT), or the locally most powerful invariant test (LMPIT), etc. Our paper closes this gap. Our approach uses the relationship between a scalar-valued CS time series and a vector-valued WSS time series [33] to formulate the problem as a test for the covariance structure of the observations. The derivation of the GLRT is relatively straightforward, and the main difficulty is that there is no closed-form maximum likelihood (ML) estimator of the covariance matrices because these are block-Toeplitz. This difficulty is addressed by considering the asymptotic case where the covariance matrices become block-circulant. The derivation of the LMPIT is a bit more involved. The typical approach for deriving the LMPIT is based on the maximal invariant statistic. Then its distribution under both hypotheses is obtained and the ratio of the distributions is calculated. If this ratio (or a transformation thereof) does not depend on unknown parameters it is the UMPIT. If it does, we may instead obtain the LMPIT for close hypotheses. Yet this approach only works for a very few selected problems. Here, we instead use Wijsman's theorem [38]–[41], which allows us to obtain the ratio of the distributions of the maximal invariant statistic without actually deriving the distributions or even the maximal invariant statistic. Incidentally, both GLRT and LMPIT are functions of coherence matrices, as are the detectors for spatial correlation in [42]–[44].

The paper is organized as follows: Section II presents the detection problem and formulates it as a test for the covariance structure of the observations. In Section III, we reformulate the problem in the frequency domain. Sections IV and V derive the GLRT and the LMPIT, respectively. An illuminating interpretation of the detectors in the Loève frequency domain is presented in Section VI. Finally, Section VII numerically evaluates the performance of our detectors.

II. Problem Formulation

We consider the problem of testing whether a zero-mean multivariate time series, observed by L sensors or antennas, is WSS, or CS with *known* cycle period P, or nonstationary (NS). That is, we are interested in the following three hypotheses:

$$\begin{aligned}&\mathcal{H}_0 : \mathbf{u}[n] \text{ is WSS},\\ &\mathcal{H}_1 : \mathbf{u}[n] \text{ is CS with period } P,\\ &\mathcal{H}_2 : \mathbf{u}[n] \text{ is NS},\end{aligned} \tag{1}$$

where $\mathbf{u}[n] \in \mathbb{C}^L$ is a multivariate process of dimension L, assumed proper complex Gaussian [45]. Given NP samples of $\mathbf{u}[n]$, which are collected in the vector

$$\mathbf{y} = [\,\mathbf{u}^T[0] \quad \mathbf{u}^T[1] \quad \cdots \quad \mathbf{u}^T[NP-1]\,]^T \in \mathbb{C}^{LNP}, \tag{2}$$

the hypotheses in (1) may be formulated as

$$\begin{aligned}&\mathcal{H}_0 : \mathbf{y} \sim \mathcal{CN}(\mathbf{0}, \mathbf{R}_0),\\ &\mathcal{H}_1 : \mathbf{y} \sim \mathcal{CN}(\mathbf{0}, \mathbf{R}_1),\\ &\mathcal{H}_2 : \mathbf{y} \sim \mathcal{CN}(\mathbf{0}, \mathbf{R}_2),\end{aligned} \tag{3}$$

where $\mathbf{R}_i \in \mathbb{C}^{LNP\times LNP}$ is the covariance matrix under the ith hypothesis. Hence the hypothesis test is based on the structure of $\mathbf{R}_i$.

The NS case is the simplest because $\mathbf{R}_2$ does not have any particular structure beyond being positive definite,

$$\mathbf{R}_2 = \begin{bmatrix} \mathbf{M}_2[0,0] & \cdots & \mathbf{M}_2[0,-NP+1] \\ \vdots & \ddots & \vdots \\ \mathbf{M}_2[NP-1,NP-1] & \cdots & \mathbf{M}_2[NP-1,0] \end{bmatrix}, \tag{4}$$

where $\mathbf{M}_2[n,m] = E[\mathbf{u}[n]\mathbf{u}^H[n-m]] \in \mathbb{C}^{L\times L}$ is the NS matrix-valued covariance sequence. The structure under stationarity is also easy to obtain [46], and the covariance matrix is

$$\mathbf{R}_0 = \begin{bmatrix} \mathbf{M}_0[0] & \cdots & \mathbf{M}_0[-NP+1] \\ \vdots & \ddots & \vdots \\ \mathbf{M}_0[NP-1] & \cdots & \mathbf{M}_0[0] \end{bmatrix}, \tag{5}$$

where $\mathbf{M}_0[m] = E[\mathbf{u}[n]\mathbf{u}^H[n-m]] \in \mathbb{C}^{L\times L}$ is the WSS matrix-valued covariance sequence. It is clear that $\mathbf{R}_0$ is block-Toeplitz with block size L (the number of antennas or sensors).

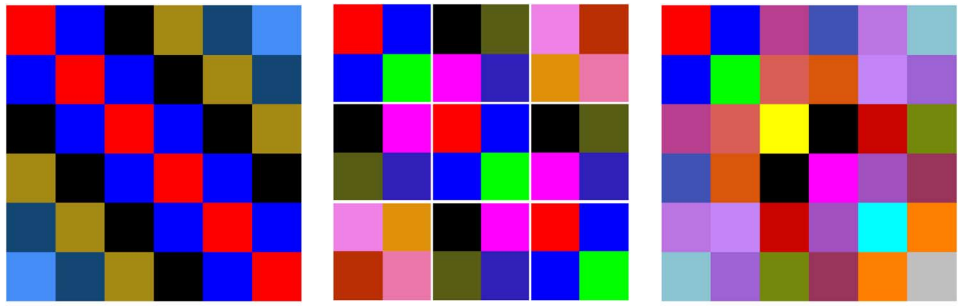

(a) (b) (c)

Fig. 1. Structure of the covariance matrix for $N = 3$ and $P = 2$ under the three considered hypotheses. Each square corresponds to an $L \times L$ matrix. (a) Stationary case; (b) Cyclostationary case; (c) Nonstationary case.

That is, the (m, l)th block is $\mathbf{M}_0[m - l]$. Finally, to find the structure of $\mathbf{R}_1$ under cyclostationarity, we follow our previous work [47]. We arrange $\mathbf{u}[n]$ in blocks of size P to obtain the time series

$$\mathbf{x}[n] = [\,\mathbf{u}^T[nP] \quad \cdots \quad \mathbf{u}^T[(n+1)P-1]\,]^T \in \mathbb{C}^{LP}, \quad (6)$$

which is WSS [33]. The vector $\mathbf{y}$ may therefore be rewritten in terms of $\mathbf{x}[n]$ as

$$\mathbf{y} = [\,\mathbf{x}^T[0] \quad \mathbf{x}^T[1] \quad \cdots \quad \mathbf{x}^T[N-1]\,]^T \in \mathbb{C}^{LNP}, \quad (7)$$

which is a stack of N samples of the WSS process $\mathbf{x}[n]$. Hence, the covariance matrix is also block-Toeplitz, but with block size LP:

$$\mathbf{R}_1 = \begin{bmatrix} \mathbf{M}_1[0] & \cdots & \mathbf{M}_1[-N+1] \\ \vdots & \ddots & \vdots \\ \mathbf{M}_1[N-1] & \cdots & \mathbf{M}_1[0] \end{bmatrix}, \quad (8)$$

where $\mathbf{M}_1[m] = E[\mathbf{x}[n]\mathbf{x}^H[n-m]] \in \mathbb{C}^{LP \times LP}$ is the matrix-valued WSS covariance sequence. To sum up, the covariance matrix is block-Toeplitz under $\mathcal{H}_0$ and $\mathcal{H}_1$, but only positive definite under $\mathcal{H}_2$ (see Fig. 1).

One final comment is in order. Only the structure of the covariance matrices is known under each of the three hypotheses, but the particular values, that is, the matrix-valued covariance sequences, are unknown. Thus, the only information available *a priori* is the cycle period.

III. Rewriting the Hypotheses: Asymptotic Case

Since the covariance matrices are unknown, the hypotheses are composite, in which case the GLRT, the UMPIT and the LMPIT are typical approaches for binary tests [48], [49]. For the GLRT we need the ML estimates of the unknown parameters, which, in our case, are the covariance matrices. As we have seen, under stationarity and cyclostationarity these covariance matrices are block-Toeplitz, for which there is no closed-form ML estimate [49]. Thus, we will follow an approach similar to the one proposed in [43], [46], [47], which enables us to derive an *asymptotic* GLRT.

Assume that we are given M independent and identically distributed (i.i.d.) realizations $\{\mathbf{y}_l\}_{m=0}^{M-1}$ of the vector $\mathbf{y}$. The likelihood of these observations under $\mathcal{H}_i$ is

$$p(\mathbf{y}_0, \ldots, \mathbf{y}_{M-1}; \mathbf{R}_i) = \prod_{m=0}^{M-1} p(\mathbf{y}_m; \mathbf{R}_i) = \frac{1}{\pi^{LNPM} \det(\mathbf{R}_i)^M} \exp\left\{-M \mathrm{tr}\left(\mathbf{R}_i^{-1}\hat{\mathbf{R}}\right)\right\}, \quad (9)$$

where the sample covariance matrix is

$$\hat{\mathbf{R}} = \frac{1}{M}\sum_{m=0}^{M-1} \mathbf{y}_m \mathbf{y}_m^H. \quad (10)$$

Since there is no closed-form solution for ML estimates of block-Toeplitz matrices we approximate them by block-circulant matrices. Block-Toeplitz matrices are asymptotically equivalent to block-circulant matrices [50], [51], and the likelihoods converge in mean-square, as shown in the following theorem.

Theorem 1: As $N \to \infty$, the log-likelihood random variable (RV), parameterized by a block-Toeplitz covariance matrix, converges in mean-square (sometimes called l.i.m.) to the log-likelihood RV parameterized by a properly selected block-circulant covariance matrix:

$$\lim_{N\to\infty} E\left[\frac{1}{N^2}\left|\log p(\mathbf{y}_0, \ldots, \mathbf{y}_{M-1}; \mathbf{R}) - \log p(\mathbf{y}_0, \ldots, \mathbf{y}_{M-1}; \mathbf{Q})\right|^2\right] = 0,$$

where $\mathbf{y}_m \in \mathbb{C}^{NB}$, and $\mathbf{R} \in \mathbb{C}^{NB \times NB}$ is the block-Toeplitz covariance matrix with a generic block size B,

$$\mathbf{R} = \begin{bmatrix} \mathbf{M}[0] & \cdots & \mathbf{M}[-N+1] \\ \vdots & \ddots & \vdots \\ \mathbf{M}[N-1] & \cdots & \mathbf{M}[0] \end{bmatrix}. \quad (11)$$

The matrix-valued covariance sequence that generates $\mathbf{R}$ is $\mathbf{M}[m] \in \mathbb{C}^{B \times B}$, and $\mathbf{Q} \in \mathbb{C}^{NB \times NB}$ is the block-circulant covariance matrix whose (m, l)th block is $\mathbf{M}[m - l \bmod N]$. Equivalently, the block-circulant matrix may be factored as

$$\mathbf{Q} = (\mathbf{F}_N \otimes \mathbf{I}_B)\mathbf{V}(\mathbf{F}_N \otimes \mathbf{I}_B)^H. \quad (12)$$

Here, $\mathbf{F}_N$ is the Fourier matrix of dimension N, and $\mathbf{V}$ is a block-diagonal matrix, whose kth block is given by the discrete Fourier transform (DFT) of the covariance sequence,

$$\mathbf{V}(\theta_k) = \sum_{m=0}^{N-1} \mathbf{M}[m] \exp\{-j\theta_k m\}, \tag{13}$$

with $\theta_k = 2\pi k/N$. Thus, $\mathbf{V}(\theta_k)$ is simply the cross-spectral matrix (CSM) at frequency θ_k.

Proof: The proof follows from [46] with a few modifications. ∎

Corollary 1: The log-likelihood for the block-circulant covariance matrix may be rewritten as

$$\log p(\mathbf{y}_0, \ldots, \mathbf{y}_{M-1}; \mathbf{Q}) = -NBM \log \pi - NM \int_0^{2\pi} \log\det \mathbf{V}(\theta) \frac{d\theta}{2\pi} - NM \int_0^{2\pi} \operatorname{tr}\left[\mathbf{V}^{-1}(\theta)\hat{\mathbf{V}}(\theta)\right] \frac{d\theta}{2\pi}, \tag{14}$$

where $\hat{\mathbf{V}}(\theta)$ is the sample CSM at frequency θ.

Taking into account Theorem 1, the hypotheses in (3) are *asymptotically* equivalent to

$$\begin{aligned} \mathcal{H}_0 &: \mathbf{y} \sim \mathcal{CN}(\mathbf{0}, \mathbf{Q}_0), \\ \mathcal{H}_1 &: \mathbf{y} \sim \mathcal{CN}(\mathbf{0}, \mathbf{Q}_1), \\ \mathcal{H}_2 &: \mathbf{y} \sim \mathcal{CN}(\mathbf{0}, \mathbf{Q}_2). \end{aligned} \tag{15}$$

For nonstationary data, $\mathbf{Q}_2$ is positive definite without further structure. For cyclostationary data, $\mathbf{Q}_1$ is block-circulant with block size LP and may therefore be factored as

$$\mathbf{Q}_1 = (\mathbf{F}_N \otimes \mathbf{I}_{LP}) \mathbf{V}_1 (\mathbf{F}_N \otimes \mathbf{I}_{LP})^H, \tag{16}$$

where $\mathbf{V}_1$ is an unknown positive definite block-diagonal matrix of block size LP. For stationary data, $\mathbf{Q}_0$ is a block-circulant covariance matrix with block size L, which may be factored as

$$\mathbf{Q}_0 = (\mathbf{F}_{NP} \otimes \mathbf{I}_L) \mathbf{V}_0 (\mathbf{F}_{NP} \otimes \mathbf{I}_L)^H, \tag{17}$$

where $\mathbf{V}_0$ is a positive definite block-diagonal matrix of block size L.

Let us now transform the observations as

$$\mathbf{z} = (\mathbf{L}_{NP,N} \otimes \mathbf{I}_L)(\mathbf{F}_{NP} \otimes \mathbf{I}_L)^H \mathbf{y}, \tag{18}$$

where $\mathbf{L}_{NP,N}$ is the commutation (or "stride permutation") matrix [52], which fulfills $\operatorname{vec}(\mathbf{A}) = \mathbf{L}_{NP,N} \operatorname{vec}(\mathbf{A}^T)$, where $\mathbf{A}$ is a $P \times N$ matrix. Basically, this transformation is a particular reordering of the frequencies in the DFT of $\mathbf{u}[n]$. We formulate the hypothesis test in terms of $\mathbf{z}$ instead of $\mathbf{y}$ and must therefore obtain the covariance matrix of $\mathbf{z}$ under the three hypotheses. Under $\mathcal{H}_2$, the covariance matrix is

$$\begin{aligned} \mathbf{S}_2 &= E[\mathbf{z}\mathbf{z}^H | \mathcal{H}_2] \\ &= \left(\mathbf{L}_{NP,N} \mathbf{F}_{NP}^H \otimes \mathbf{I}_L\right) \mathbf{Q}_2 \left(\mathbf{F}_{NP} \mathbf{L}_{NP,N}^T \otimes \mathbf{I}_L\right), \end{aligned} \tag{19}$$

which is another unknown positive definite matrix. Under $\mathcal{H}_0$, the covariance matrix of the transformed observations is

$$\mathbf{S}_0 = \left(\mathbf{L}_{NP,N} \mathbf{F}_{NP}^H \otimes \mathbf{I}_L\right) \mathbf{Q}_0 \left(\mathbf{F}_{NP} \mathbf{L}_{NP,N}^T \otimes \mathbf{I}_L\right), \tag{20}$$

and, taking into account (17),

$$\mathbf{S}_0 = (NP)^2 (\mathbf{L}_{NP,N} \otimes \mathbf{I}_L) \mathbf{V}_0 (\mathbf{L}_{NP,N} \otimes \mathbf{I}_L)^T, \tag{21}$$

where we have used $(\mathbf{F}_{NP} \otimes \mathbf{I}_L)^H (\mathbf{F}_{NP} \otimes \mathbf{I}_L) = NP\mathbf{I}_{LNP}$. Thus, the covariance matrix is just a scaled and permuted version of the blocks of $\mathbf{V}_0$, and since $\mathbf{V}_0$ is unknown, $\mathbf{S}_0$ is also an unknown positive definite block-diagonal matrix. Under $\mathcal{H}_1$, the derivation is more involved and based on the Cooley-Tukey theorem.

Theorem 2 (Cooley-Tukey): The Fourier matrix may be factored as

$$\mathbf{F}_{NP} = (\mathbf{F}_N \otimes \mathbf{I}_P) \mathbf{T}_{NP,P} (\mathbf{I}_N \otimes \mathbf{F}_P) \mathbf{L}_{NP,N}, \tag{22}$$

where $\mathbf{T}_{NP,P}$ is a diagonal matrix of twiddle factors.

Proof: See [53]. ∎

The covariance matrix under $\mathcal{H}_1$ is given by

$$\mathbf{S}_1 = \left(\mathbf{L}_{NP,N} \mathbf{F}_{NP}^H \otimes \mathbf{I}_L\right) \mathbf{Q}_1 \left(\mathbf{F}_{NP} \mathbf{L}_{NP,N}^T \otimes \mathbf{I}_L\right), \tag{23}$$

and, using the factorization in (16), it becomes

$$\begin{aligned} \mathbf{S}_1 = \left(\mathbf{L}_{NP,N} \mathbf{F}_{NP}^T \otimes \mathbf{I}_L\right) &(\mathbf{F}_N \otimes \mathbf{I}_{LP}) \\ &\times \mathbf{V}_1 (\mathbf{F}_N \otimes \mathbf{I}_{LP})^H \left(\mathbf{F}_{NP} \mathbf{L}_{NP,N}^T \otimes \mathbf{I}_L\right). \end{aligned} \tag{24}$$

With

$$\mathbf{F}_N \otimes \mathbf{I}_{LP} = (\mathbf{F}_N \otimes \mathbf{I}_P) \otimes \mathbf{I}_L \tag{25}$$

and the associative property of the Kronecker product, we obtain

$$\begin{aligned} \left(\mathbf{L}_{NP,N} \mathbf{F}_{NP}^H \otimes \mathbf{I}_L\right) &(\mathbf{F}_N \otimes \mathbf{I}_{LP}) = \\ &\left[\mathbf{L}_{NP,N} \mathbf{F}_{NP}^H (\mathbf{F}_N \otimes \mathbf{I}_P)\right] \otimes \mathbf{I}_L. \end{aligned} \tag{26}$$

Applying Theorem 2, the term inside the square brackets becomes

$$\mathbf{L}_{NP,N} \mathbf{F}_{NP}^H (\mathbf{F}_N \otimes \mathbf{I}_P) = N (\mathbf{I}_N \otimes \mathbf{F}_P)^H \mathbf{T}_{NP,P}^*, \tag{27}$$

which yields

$$\begin{aligned} \mathbf{S}_1 = N^2 &\left[(\mathbf{I}_N \otimes \mathbf{F}_P)^H \mathbf{T}_{NP,P}^*\right] \otimes \mathbf{I}_L \\ &\times \mathbf{V}_1 \left[\mathbf{T}_{NP,P} (\mathbf{I}_N \otimes \mathbf{F}_P)\right] \otimes \mathbf{I}_L. \end{aligned} \tag{28}$$

It is clear that the Kronecker product of the matrix inside the square brackets and the identity matrix results in a block-diagonal matrix with block size LP. Since the covariance matrix under $\mathcal{H}_1$ is an unknown positive definite block-diagonal matrix multiplied on the left by a block-diagonal matrix with the same block size and on the right by the Hermitian transpose of this matrix, $\mathbf{S}_1$ is also an unknown positive definite block-diagonal matrix with block size LP.

Putting all the pieces together, the hypotheses are

$$\begin{aligned} \mathcal{H}_0 &: \mathbf{z} \sim \mathcal{CN}(\mathbf{0}, \mathbf{S}_0), \\ \mathcal{H}_1 &: \mathbf{z} \sim \mathcal{CN}(\mathbf{0}, \mathbf{S}_1), \\ \mathcal{H}_2 &: \mathbf{z} \sim \mathcal{CN}(\mathbf{0}, \mathbf{S}_2), \end{aligned} \tag{29}$$

where $\mathbf{S}_2$ is a positive definite matrix without further structure, $\mathbf{S}_1$ is a positive definite block-diagonal matrix with block size LP, and $\mathbf{S}_0$ is also a positive definite block-diagonal matrix but with block size L. Hence, under all three hypotheses, the covariance matrices are block-diagonal. $\mathbf{S}_2$ contains just one block of size $LPN \times LPN$. This fact will simplify the derivations of the tests. Moreover, an insightful interpretation of these covariance matrices is presented in Section VI.

IV. Derivation of the GLRT

In the previous section, we showed that the three covariance matrices are block-diagonal without further structure but different block sizes. In this section, we derive the GLRT for the case of two block-diagonal with arbitrary block sizes. Later on, these block sizes are chosen as those in (29) to derive the asymptotic GLRT for the tests CS vs. WSS signals, and CS vs. NS signals. The derivation of the LMPIT follows in Section VI.

A. GLRT for Block-Diagonality With Different Block Sizes

Consider the following hypothesis test

$$\begin{aligned} \mathcal{H}_0 &: \mathbf{z} \sim \mathcal{CN}(\mathbf{0}, \mathbf{D}_0), \\ \mathcal{H}_1 &: \mathbf{z} \sim \mathcal{CN}(\mathbf{0}, \mathbf{D}_1), \end{aligned} \tag{30}$$

where $\mathbf{D}_0$ is a block-diagonal matrix with block size B_0 and without further structure, i.e. $\mathbf{D}_0 \in \mathbb{S}_{B_0}$, and $\mathbf{D}_1$ is a block-diagonal matrix with block size B_1 and without further structure, i.e. $\mathbf{D}_1 \in \mathbb{S}_{B_1}$. Of course, B_1 must be a multiple of B_0 because the sizes of $\mathbf{D}_1$ and $\mathbf{D}_0$ are the same.

The generalized likelihood ratio (GLR) for the test in (30) is given by

$$\mathcal{G} = \frac{\max\limits_{\mathbf{D}_0 \in \mathbb{S}_{B_0}} p(\mathbf{z}_0, \ldots, \mathbf{z}_{M-1}; \mathbf{D}_0)}{\max\limits_{\mathbf{D}_1 \in \mathbb{S}_{B_1}} p(\mathbf{z}_0, \ldots, \mathbf{z}_{M-1}; \mathbf{D}_1)} \tag{31}$$

where the maximization is carried out over the set of positive definite block-diagonal matrices, with block size B_0 under $\mathcal{H}_0$ and block size B_1 under $\mathcal{H}_1$. In the following theorem we present the solution to (31).

Theorem 3: The GLRT in (31) is

$$\mathcal{G}^{\frac{1}{M}} = \frac{\det(\mathrm{diag}_{B_1}(\hat{\mathbf{S}}))}{\det(\mathrm{diag}_{B_0}\left(\hat{\mathbf{S}}\right)} = \det\left(\hat{\mathbf{C}}_{B_0}^{B_1}\right), \tag{32}$$

where $\mathrm{diag}_{B_i}(\hat{\mathbf{S}})$, $i = 0, 1$, builds a block-diagonal matrix from the $B_i \times B_i$ blocks on the main diagonal of $\hat{\mathbf{S}}$ by setting the off-diagonal blocks equal to zero, $\hat{\mathbf{C}}_{B_0}^{B_1} = [\mathrm{diag}_{B_0}(\hat{\mathbf{S}})]^{-1/2}\mathrm{diag}_{B_1}(\hat{\mathbf{S}})[\mathrm{diag}_{B_0}(\hat{\mathbf{S}})]^{-1/2}$ is a *coherence matrix*, and $\hat{\mathbf{S}}$ is the sample covariance matrix of $\mathbf{z}_0, \ldots, \mathbf{z}_{M-1}$.

Proof: Under both hypotheses, we need the ML estimate of a block-diagonal covariance matrix. The likelihood for a generic block size B is given by

$$p(\mathbf{z}_0, \ldots, \mathbf{z}_{M-1}; \mathbf{D}) = \frac{1}{\pi^{NBM}\det(\mathbf{D})^M} \exp\left\{-M\mathrm{tr}(\mathbf{D}^{-1}\hat{\mathbf{S}})\right\}. \tag{33}$$

Taking into account the block-diagonal structure of $\mathbf{D}$, the likelihood becomes

$$p(\mathbf{z}_0, \ldots, \mathbf{z}_{M-1}; \mathbf{D}) = \prod_{k=1}^{N} \frac{1}{\pi^{BM}\det(\mathbf{D}_k)^M} \exp\left\{-M\mathrm{tr}\left(\mathbf{D}_k^{-1}\hat{\mathbf{S}}_k\right)\right\}, \tag{34}$$

where $\mathbf{D}_k$ and $\hat{\mathbf{S}}_k$ are the kth blocks of dimensions $B \times B$ on the diagonal of $\mathbf{D}$ and $\hat{\mathbf{S}}$, respectively. Since $\mathbf{D}_k$ has no structure besides being positive definite, its ML estimate is $\hat{\mathbf{D}}_k = \hat{\mathbf{S}}_k$, which is easily proven using the derivatives in [54]. Finally, the proof is concluded by building a block-diagonal matrix with blocks $\hat{\mathbf{S}}_k$, with $k = 1, \ldots, N$, which yields

$$\hat{\mathbf{D}} = \mathrm{diag}_B(\hat{\mathbf{S}}). \tag{35}$$

Applying the ML estimator in (35) directly to the block-diagonal matrices in (30), and plugging these back into (31), the proof follows. ∎

B. GLRT for Testing Cyclostationarity vs. Wide-Sense Stationarity

The generalized likelihood ratio (GLR) for testing cyclostationarity vs. wide-sense stationarity is

$$\mathcal{G}_{0:1} = \frac{\max\limits_{\mathbf{S}_0 \in \mathbb{S}_L} p(\mathbf{z}_0, \ldots, \mathbf{z}_{M-1}; \mathbf{S}_0)}{\max\limits_{\mathbf{S}_1 \in \mathbb{S}_{LP}} p(\mathbf{z}_0, \ldots, \mathbf{z}_{M-1}; \mathbf{S}_1)}, \tag{36}$$

for which we may use the results in the previous subsection. The solution is presented in the following theorem.

Theorem 4: Asymptotically, as $N \to \infty$, the GLR for the test $\mathcal{H}_0$ vs. $\mathcal{H}_1$ is

$$\mathcal{G}_{0:1}^{\frac{1}{M}} = \frac{\det\left(\mathrm{diag}_{LP}(\hat{\mathbf{S}})\right)}{\det\left(\mathrm{diag}_{L}(\hat{\mathbf{S}})\right)} = \det\left(\hat{\mathbf{C}}_L^{LP}\right) = \prod_{k=1}^{N}\det(\hat{\mathbf{C}}_k), \tag{37}$$

where $\hat{\mathbf{C}}_L^{LP} = [\mathrm{diag}_L(\hat{\mathbf{S}})]^{-1/2}\mathrm{diag}_{LP}(\hat{\mathbf{S}})[\mathrm{diag}_L(\hat{\mathbf{S}})]^{-1/2}$ is a coherence matrix, and the kth $LP \times LP$ block on the diagonal of $\hat{\mathbf{C}}_L^{LP}$ is denoted by $\hat{\mathbf{C}}_k$.

Proof: The proof is a direct application of the GLRT in the previous subsection. ∎

It is clear that $\mathcal{G}_{0:1}$ is invariant to multiplications by a nonsingular block-diagonal matrix with block size L. This means the GLRT is asymptotically invariant to multiplications in the frequency domain, hence invariant to MIMO linear filtering (circular convolution) of $\mathbf{u}[n]$. For finite N, this invariance only holds approximately.

Interestingly, using the properties of the determinant, the above GLRT may be rewritten as

$$\log \mathcal{G}_{0:1} = \int_0^{2\pi} \log\det \hat{\mathbf{V}}_1(\theta)\frac{d\theta}{2\pi} - P\int_0^{2\pi} \log\det \hat{\mathbf{V}}_0(\theta)\frac{d\theta}{2\pi}, \tag{38}$$

where $\hat{\mathbf{V}}_1(\theta)$ is the estimate of the CSM of the WSS vector representation $\mathbf{x}[n]$, given by

$$\hat{\mathbf{V}}_1(\theta) = \frac{1}{M}\sum_{m=0}^{M-1} \mathbf{x}_m(\theta)\mathbf{x}_m^H(\theta), \tag{39}$$

where

$$\mathbf{x}_m(\theta) = \frac{1}{\sqrt{N}} \sum_{n=0}^{N-1} \mathbf{x}_m[n] e^{-j\theta n}. \tag{40}$$

Similarly, $\hat{\mathbf{V}}_0(\theta)$ is the estimate of the CSM of $\mathbf{u}[n]$, given by

$$\hat{\mathbf{V}}_0(\theta) = \frac{1}{M} \sum_{m=0}^{M-1} \mathbf{u}_m(\theta) \mathbf{u}_m^H(\theta), \tag{41}$$

with

$$\mathbf{u}_m(\theta) = \frac{1}{\sqrt{NP}} \sum_{n=0}^{NP-1} \mathbf{u}_m[n] e^{-j\theta n}. \tag{42}$$

For the scalar case, $L = 1$, this GLRT was derived in [47].

C. GLRT for Testing Cyclostationarity vs. Nonstationarity

For the test $\mathcal{H}_1$ against $\mathcal{H}_2$, the GLR is

$$\mathcal{G}_{1:2} = \frac{\max\limits_{\mathbf{S}_1 \in \mathbb{S}_{LP}} p(\mathbf{z}_0, \ldots, \mathbf{z}_{M-1}; \mathbf{S}_1)}{\max\limits_{\mathbf{S}_2 \in \mathbb{S}} p(\mathbf{z}_0, \ldots, \mathbf{z}_{M-1}; \mathbf{S}_2)}, \tag{43}$$

and the solution is presented next.

Theorem 5: Asymptotically, as $N \to \infty$, the GLR for the test $\mathcal{H}_2$ vs. $\mathcal{H}_1$ is

$$\mathcal{G}_{1:2}^{\frac{1}{M}} = \frac{\det(\hat{\mathbf{S}})}{\det\left(\mathrm{diag}_{LP}(\hat{\mathbf{S}})\right)} = \det\left(\hat{\mathbf{C}}_{LP}^{LPN}\right), \tag{44}$$

where $\hat{\mathbf{C}}_{LP}^{LPN} = [\mathrm{diag}_{LP}(\hat{\mathbf{S}})]^{-1/2} \hat{\mathbf{S}} [\mathrm{diag}_{LP}(\hat{\mathbf{S}})]^{-1/2}$ is a coherence matrix.

Proof: The proof is a direct application of Theorem 3. ■

We note that while the ML estimate of $\mathbf{S}_1$ is an asymptotic estimate, the estimate $\mathbf{S}_2$ is an ML estimate for finite values of N, provided that $M \geq LNP$. Moreover, the GLRT is invariant to multiplications by any nonsingular block-diagonal matrix with block size LP. Hence, the GLRT for $\mathcal{H}_1$ vs. $\mathcal{H}_2$ is asymptotically invariant to linear filtering (circular convolution) of $\mathbf{x}[n]$ (rather than $\mathbf{u}[n]$ when testing $\mathcal{H}_1$ vs. $\mathcal{H}_0$).

Finally, it is also worth noting that this approach can be used to show that the GLR for the test WSS vs. NS is $\det(\hat{\mathbf{C}}_L^{LPN})$. However, we do not consider this test in more detail since it is outside the scope of the paper.

V. Derivation of the LMPIT

In this section, as in the previous one, we test block-diagonality with two different block sizes, but now using the LMPIT. To do so, we first study the invariances of the hypothesis test and use those to derive the LMPIT. We employ Wijsman's theorem to avoid having to derive the maximal invariant statistic and its distributions. For a more detailed review of Wijsman's theorem, see Appendix A. Then, the aforementioned LMPIT is particularized to the tests cyclostationarity vs. wide-sense stationarity and cyclostationarity vs. nonstationarity.

A. LMPIT for Block-Diagonality With Different Block Sizes

In this subsection we derive the LMPIT for the test in (30), and we use this LMPIT to obtain the asymptotic LMPITs for testing cyclostationarity vs. wide-sense stationarity and cyclostationarity vs. nonstationarity. The first step is to find the invariances of the detection problem. First, we may restrict our attention to linear operations since Gaussianity must be preserved. We may also multiply $\mathbf{z}$ by any nonsingular block-diagonal matrix, with block size B_0, without modifying the structure of the hypothesis test. Moreover, we can permute blocks of size B_1 without modifying the block-diagonal structure of $\mathbf{D}_1$, and within these $B_1 \times B_1$ blocks, it is also possible to permute blocks of size B_0 without modifying the block-diagonal structure of $\mathbf{D}_0$. Therefore, the invariance group is

$$\mathcal{G} = \{g : \mathbf{z} \to g(\mathbf{z}) = \mathbf{P}\mathbf{G}\mathbf{z},\ \mathbf{P} = \mathbf{P}_\kappa \otimes (\mathbf{P}_\mu \otimes \mathbf{I}_{B_0})\}, \tag{45}$$

where $\mathbf{P}_\kappa \in \mathbb{P}_\kappa$, $\mathbf{P}_\mu \in \mathbb{P}_\mu$, $\mathbf{G} \in \mathbb{D}_{B_0}$, $\mathbb{P}_\kappa$ denotes the set of κ-dimensional permutation matrices and $\mathbb{D}_{B_0}$ is the set of nonsingular block-diagonal matrices with block size B_0. Here, κ is the ratio between the size of the covariance matrices and B_1, that is, the number of blocks of dimension $B_1 \times B_1$, and μ is the ratio between B_1 and B_0, that is, the number of blocks of dimension $B_0 \times B_0$ that forms a block of size $B_1 \times B_1$.

Given this invariance group, Wijsman's theorem [38] allows us to write the ratio of the distributions of the maximal invariant statistic shown in (46) at the bottom of the page. In (46) we sum over all possible permutations since the permutation group is a finite group. In its current form, $\mathcal{L}$ is a function of the unknown parameters, which prevents the derivation of the UMPIT or LMPIT. In the following, we will simplify this expression to derive the LMPIT.

Lemma 1: The ratio $\mathcal{L}$ may be simplified to

$$\mathcal{L} \propto \sum_{\mathbb{P}_\kappa, \mathbb{P}_\mu} \int_{\mathbb{D}_{B_0}} \beta(\mathbf{G}) e^{-\alpha} d\mathbf{G}, \tag{47}$$

where $\beta(\mathbf{G}) = |\det(\mathbf{G})^{2M}| e^{-M\mathrm{tr}(\mathbf{G}\mathbf{G}^H)}$ and

$$\alpha = M \sum_{k=1}^{\kappa} \sum_{\substack{l,m=1 \\ l \neq m}}^{\mu} \mathrm{tr}\left(\tilde{\mathbf{D}}_k^{(lm)} \mathbf{G}_k^{(m)} \hat{\mathbf{C}}_k^{(ml)} \mathbf{G}_k^{(l)H}\right). \tag{48}$$

Here $\mathbf{G}_k$ is the kth $B_1 \times B_1$ block on the diagonal of $\mathbf{G}$, which is also block-diagonal with $B_0 \times B_0$ blocks $\mathbf{G}_k^{(l)}$. The coherence matrix $\hat{\mathbf{C}}_{B_0}^{B_1}$ is defined in the previous section, and it is a block-

$$\mathcal{L} = \frac{\sum\limits_{\mathbb{P}_\kappa, \mathbb{P}_\mu} \int_{\mathbb{D}_{B_0}} \det(\mathbf{D}_1)^{-M} \left|\det(\mathbf{G})^{2M}\right| \exp\left[-M\mathrm{tr}\left(\mathbf{D}_1^{-1} \mathbf{P}\mathbf{G}\hat{\mathbf{S}}\mathbf{G}^H\mathbf{P}^T\right)\right] d\mathbf{G}}{\sum\limits_{\mathbb{P}_\kappa, \mathbb{P}_\mu} \int_{\mathbb{D}_{B_0}} \det(\mathbf{D}_0)^{-M} \left|\det(\mathbf{G})^{2M}\right| \exp\left[-M\mathrm{tr}\left(\mathbf{D}_0^{-1} \mathbf{P}\mathbf{G}\hat{\mathbf{S}}\mathbf{G}^H\mathbf{P}^T\right)\right] d\mathbf{G}}, \tag{46}$$

diagonal matrix, with block size B_1. The kth block is denoted by[1] $\hat{\mathbf{C}}_k$, which is itself a block matrix with $B_0 \times B_0$ blocks denoted by $\hat{\mathbf{C}}_k^{(ml)}$. Finally, $\tilde{\mathbf{D}}_k$ is the kth $B_1 \times B_1$ block on the diagonal of

$$\tilde{\mathbf{D}} = \mathbf{P}^T \left(\text{diag}_{B_0}\left(\mathbf{D}_1^{-1}\right)\right)^{-1/2} \mathbf{D}_1^{-1} \left(\text{diag}_{B_0}\left(\mathbf{D}_1^{-1}\right)\right)^{-1/2} \mathbf{P}, \tag{49}$$

and $\tilde{\mathbf{D}}_k^{(lm)}$ denotes the (l,m)th block of $\tilde{\mathbf{D}}_k$ of size $B_0 \times B_0$.

Proof: See Appendix B. ∎

We may now present the LMPIT in the following theorem.

Theorem 6: The LMPIT statistic for the test in (30) is

$$\mathcal{L} \propto \sum_{k=1}^{\kappa} \|\hat{\mathbf{C}}_k\|^2. \tag{50}$$

Proof: See Appendix C. ∎

B. LMPIT for Testing Cyclostationarity vs. Wide-Sense Stationarity

We present next the asymptotic LMPIT for testing cyclostationarity vs. wide-sense stationarity.

Theorem 7: Asymptotically, as $N \to \infty$, the LMPIT statistic for testing $\mathcal{H}_0$ vs. $\mathcal{H}_1$ is

$$\mathcal{L}_{0:1} \propto \sum_{k=1}^{N} \|\hat{\mathbf{C}}_k\|^2, \tag{51}$$

where $\hat{\mathbf{C}}_k$ is the kth block of $\hat{\mathbf{C}}_L^{LP}$, which is defined in Section IV.

Proof: Particularize the LMPIT in Theorem 6 to $B_1 = LP$, and $B_0 = L$. ∎

Again, the LMPIT is invariant to MIMO linear filtering (circular convolution) of the sequence $\mathbf{u}[n]$, which shows that the detection problem does not depend on the particular cross-spectral matrix (CSM) of $\mathbf{u}[n]$.

The LMPIT in Theorem 7 is similar in form to the LMPIT in [30] but there are differences worth mentioning. First, the derivations are different: We used the relationship between a scalar-valued CS process and a vector-valued WSS process, whereas [30] works in the frequency domain. Moreover, we consider the general multivariate case $L \geq 1$ and an arbitrary CSM under $\mathcal{H}_0$, whereas [30] treats the scalar case $L = 1$ and assumes a white process under the null hypothesis.

C. LMPIT for Testing Cyclostationarity vs. Nonstationarity

Theorem 8: Asymptotically, as $N \to \infty$, the LMPIT statistic for testing cyclostationarity vs. nonstationarity is

$$\mathcal{L}_{1:2} \propto \left\|\hat{\mathbf{C}}_{LP}^{LPN}\right\|^2. \tag{52}$$

where the coherence matrix $\hat{\mathbf{C}}_{LP}^{LPN}$ is defined in Section IV.

Proof: The proof is a direct application of Theorem 6. Alternatively, it may also be proven using the results in [44]. ∎

Similarly to the GLRT, the LMPIT is invariant to MIMO linear filtering (circular convolution) of $\mathbf{x}[n]$, rather than $\mathbf{u}[n]$. This invariance allows us to whiten the cyclic CSM, which shows that the detector cannot be a function of the cyclic CSM.

[1]Note that for the sake of notational simplicity, when there is no confussion, we drop the super-index B_1 and sub-index B_0.

VI. Interpretation of the Detectors

In this section we give an insightful interpretation of the GLRT and LMPIT in the frequency domain, for the test CS vs. WSS signals. Unfortunately, the other hypothesis test CS vs. NS signals does not easily admit an illuminating interpretation. Let us start with the covariance matrix of $\mathbf{z}$, and its relationship to the Loève spectrum and the cyclic CSM. Recall that the transformation

$$\tilde{\mathbf{z}} = (\mathbf{F}_{NP} \otimes \mathbf{I}_L)^H \mathbf{y} \in \mathbb{C}^{LNP} \tag{53}$$

is a column vector containing L-dimensional DFTs $\mathbf{u}(\theta_k) \in \mathbb{C}^L$ of the sequence $\mathbf{u}[n]$, $k = 0, 1, \ldots, NP-1$. Hence, its covariance matrix contains samples of the Loève spectrum, with the (k,l)th block of dimension $L \times L$ given by

$$\tilde{\mathbf{S}}_{k,l} = E\left[\mathbf{u}(\theta_k)\mathbf{u}^H(\theta_l)\right] = \mathbf{S}(\theta_k, \theta_l), \tag{54}$$

where $\mathbf{S}(\theta_k, \theta_l) \in \mathbb{C}^{L \times L}$ is the Loève spectrum of $\mathbf{u}[n]$ at frequencies θ_k and θ_l. To study the effect of the commutation matrix, let us rewrite the indices of the blocks of $\tilde{\mathbf{S}}$ as

$$k = i_2^{(k)} N + i_1^{(k)}, \qquad l = i_2^{(l)} N + i_1^{(l)}, \tag{55}$$

where $i_2^{(k)}, i_2^{(l)} = 0, \ldots, P-1$, and $i_1^{(k)}, i_1^{(l)} = 0, \ldots, N-1$. According to [55], the commutation matrix permutes the indices as

$$k \to k' = i_1^{(k)} P + i_2^{(k)}, \tag{56}$$

$$l \to l' = i_1^{(l)} P + i_2^{(l)}, \tag{57}$$

and the blocks of $\mathbf{S}$ become

$$\mathbf{S}_{i_1^{(k)} P + i_2^{(k)}, i_1^{(l)} P + i_2^{(l)}} = \mathbf{S}(\theta_k, \theta_l), \tag{58}$$

where

$$\theta_k = \frac{2\pi\left(i_2^{(k)} N + i_1^{(k)}\right)}{NP}, \quad \theta_l = \frac{2\pi\left(i_2^{(l)} N + i_1^{(l)}\right)}{NP}. \tag{59}$$

Thus, the matrix $\mathbf{S}$ is composed of $N \times N$ blocks of size $P \times P$, where each element is a matrix of size $L \times L$.

Now we look at the matrices $\mathbf{D}_{LP}$ and $\mathbf{D}_L$. The former is a block-diagonal matrix with block size LP and is composed by the blocks of $\mathbf{S}$ that correspond to $i_1^{(k)} = i_1^{(l)}$, i.e., $\mathbf{S}(\theta_k, \theta_l)$ with

$$\theta_k - \theta_l = \frac{2\pi}{P}\left(i_2^{(k)} - i_2^{(l)}\right).$$

That is, the blocks of $\text{diag}_{LP}(\mathbf{S})$ are the Loève spectrum with the frequencies separated by a multiple of $2\pi/P$. On the other hand, $\mathbf{D}_L$ is also block-diagonal but with block size L and it corresponds to the set of indices $i_1^{(k)} = i_1^{(l)}$ and $i_2^{(k)} = i_2^{(l)}$, which is $\mathbf{S}(\theta_l, \theta_l)$. Let us now analyze the Loève spectrum for these separations between the frequencies. The cyclic PSD

$$\mathbf{S}^{(c)}(\theta) = \sum_m \mathbf{R}^{(c)}[m] e^{-j\theta m} \tag{60}$$

with *cycle frequency* c and global frequency θ is the discrete-time Fourier transform of the cyclic covariance function

$$\mathbf{R}^{(c)}[m] = \sum_n E\left[\mathbf{u}[n]\mathbf{u}^H[n-m]\right] e^{-j2\pi cn/P}, \tag{61}$$

which in turn is the discrete Fourier series (DFS) in n of the periodic covariance sequence $E[\mathbf{u}[n]\mathbf{u}^H[n-m]]$. For CS processes, the Loève spectrum and the cyclic PSD are connected as [33]

$$\mathbf{S}(\theta_k,\theta_l)=\sum_{c=0}^{P-1}\mathbf{S}^{(c)}(\theta_l)\delta(\theta_k-\theta_l-2\pi c/P). \tag{62}$$

The support of $\mathbf{S}(\theta_k,\theta_l)$ is on the lines $\theta_k-\theta_l=2\pi c/P$, that is, harmonics of the fundamental cycle frequency. Moreover, for $\theta_k-\theta_l=0$ we have $\mathbf{S}(\theta_l,\theta_l)=\mathbf{S}^{(0)}(\theta_l)=\mathbf{S}(\theta_l)$, which is the PSD. We conclude that $\mathbf{D}_{LP}$ contains samples of $\mathbf{S}^{(c)}(\theta_l)$ for $c=-P+1,\ldots,P-1$ and $\theta_l=0,2\pi/NP,\ldots,2\pi(NP-1)/NP$, and $\mathbf{D}_L$ contains samples of $\mathbf{S}(\theta_l)$ for $\theta_l=0,2\pi/NP,\ldots,2\pi(NP-1)/NP$.

Taking all of the above into account, the matrix $\hat{\mathbf{C}}_L^{LP}$ contains blocks of the form

$$\hat{\mathbf{C}}^{(c)}(\theta_l)=\hat{\mathbf{S}}^{-1/2}(\theta_l)\hat{\mathbf{S}}^{(c)}(\theta_l)\hat{\mathbf{S}}^{-1/2}\left(\theta_l-\frac{2\pi c}{P}\right), \tag{63}$$

which will allow an insightful interpretation.[2] We start by rewriting the cyclic PSD as [45]

$$\mathbf{S}^{(c)}(\theta)d\theta=E\left[d\boldsymbol{\xi}(\theta)d\boldsymbol{\xi}^H\left(\theta+\frac{2\pi c}{P}\right)\right], \tag{64}$$

where $d\boldsymbol{\xi}(\theta)$ is an increment of the complex spectral process $\boldsymbol{\xi}(\theta)$ that generates the time series

$$\mathbf{u}[n]=\int d\boldsymbol{\xi}(\theta)e^{j\theta n}. \tag{65}$$

Thus, we conclude that $\hat{\mathbf{C}}^{(c)}(\theta_l)$ is the coherence matrix of the random vectors $d\boldsymbol{\xi}(\theta_l)$ and $d\boldsymbol{\xi}(\theta_l-2\pi c/P)$, which is illustrated in Fig. 2. For CS processes, frequencies that are separated by a multiple of the cyclic frequency are correlated, and this coherence matrix is therefore nonzero. On the other hand, for WSS processes, the coherence matrix is zero for $c\neq 0$.

The test CS vs. WSS signals is thus a test for the strength of the cyclic components relative to the WSS component in the estimated Loève spectrum. The GLRT and LMPIT differ in how they measure this relative strength, as they employ different functions of $\hat{\mathbf{C}}_L^{LP}$. The LMPIT uses the Frobenius norm

$$\mathcal{L}_{0:1}\propto\sum_{c=1}^{P-1}\sum_{l=0}^{(P-c)N-1}\left\|\hat{\mathbf{C}}^{(c)}(\theta_l)\right\|^2 \tag{66}$$

with

$$\theta_l=\frac{2\pi l}{NP}, \tag{67}$$

which, asymptotically, may be written as

$$\mathcal{L}_{0:1}\propto\sum_{c=1}^{P-1}\int_0^{\frac{2\pi(P-c)}{P}}\left\|\hat{\mathbf{C}}^{(c)}(\theta)\right\|^2\frac{d\theta}{2\pi}. \tag{68}$$

[2]Unfortunately, it does not seem possible to rewrite the matrix $\hat{\mathbf{C}}_{LP}^{LPN}$ (involved in testing CS vs. NS signals) in a similarly insightful manner.

[3]This is actually a generalized almost cyclostationary process [56], [57], which for our purposes may be considered as a NS process. For a more detailed review of this kind of process, see [58].

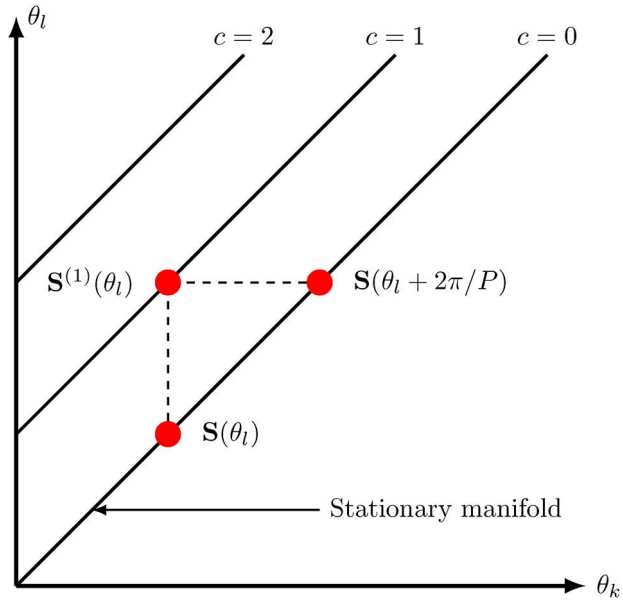

Fig. 2. Graphical representation of the coherence matrix in the Loève spectrum. Only the positive cycle frequencies are shown.

The GLRT, on the other hand, uses the determinant, which is given by a complicated nonlinear function of $\hat{\mathbf{C}}^{(c)}(\theta_l)$.

We note that the detector in [23] uses (63) as its statistic, but considers only the scalar case $L=1$. More critically, [23] uses only the fundamental cycle frequency $c=1$ and only one global frequency θ_l, instead of combining the information from all global frequencies and all harmonics of the fundamental cycle frequency.

VII. Numerical Simulations

In this section we evaluate the performance of our detectors using computer simulations. We consider a cognitive radio experiment. Our detectors can exploit the cyclostationarity induced by the symbol rate and/or the carrier frequency provided that the cycle period is known. This requires frequency synchronization and knowledge of the symbol rate. Assuming frequency synchronization and knowledge of the symbol rate, we may formulate the problem as

$$\begin{aligned}\mathcal{H}_0&:\mathbf{u}[n]=\mathbf{w}[n],\\ \mathcal{H}_1&:\mathbf{u}[n]=(\mathbf{H}*\mathbf{s})[n]+\mathbf{w}[n],\\ \mathcal{H}_2&:\mathbf{u}[n]=(\mathbf{H}_d*\mathbf{s})[n]+\mathbf{w}[n],\end{aligned} \tag{69}$$

and $\mathbf{u}[n]\in\mathbb{C}^L$ is additive Gaussian noise, which is a WSS process generated by a moving average model of order 19. The signal $\mathbf{s}[n]\in\mathbb{C}^L$ is a QPSK signal with rectangular shaping and a symbol rate of $R_s=300$ Kbauds. The channel $\mathbf{H}[n]\in\mathbb{C}^{L\times L}$ is a Rayleigh channel without correlation among antennas, it has an exponential power delay profile with a maximum delay of 24 μs, and a delay spread of 6.24 μs. The channel $\mathbf{H}_d[n]$ is time-varying due to the Doppler effect, which we generate with a normalized (to R_s) Doppler frequency of 10^{-1} and a Jakes spectrum. This makes $\mathbf{u}[n]$ NS under $\mathcal{H}_2$.[3] The sampling frequency is 1.2 MHz, which yields the cycle period $P=4$, and

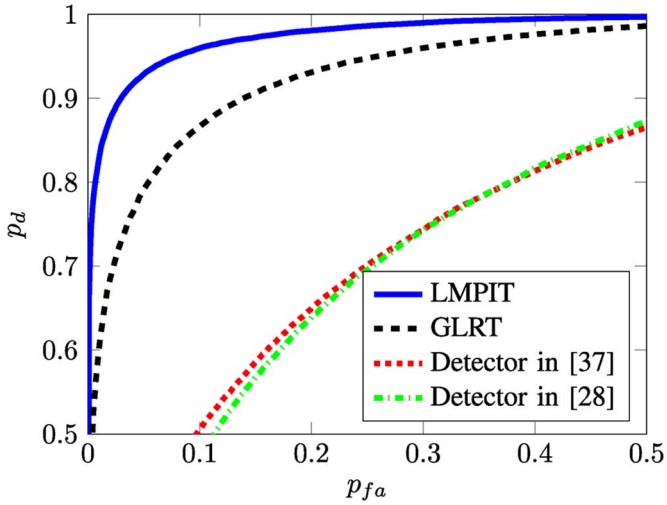

Fig. 3. ROC curves for the test CS vs. WSS in a scenario with $L = 3$, $N = 256$, $P = 4$, $M = 15$, and SNR $= -16$ dB.

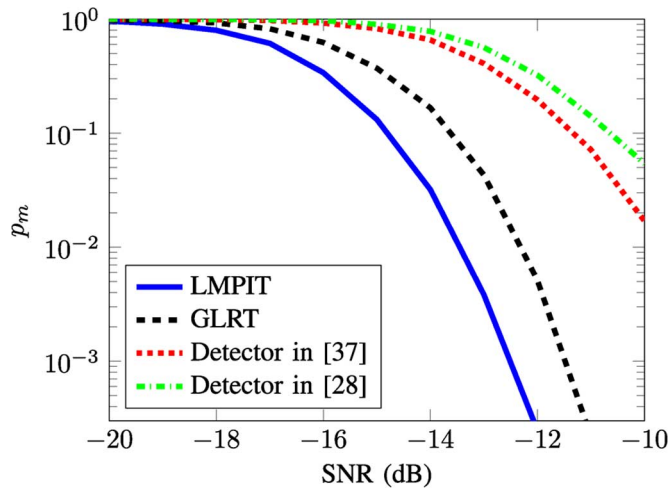

Fig. 4. Probability of missed detection vs. SNR for the test CS vs. WSS in a scenario with $L = 3$, $N = 256$, $P = 4$, and $M = 15$. The probability of false alarm is fixed at $p_{fa} = 10^{-3}$.

the channel and noise coefficients are Gaussian and randomly generated in each Monte Carlo simulation. One final comment is in order. In these simulations we have considered a communications example. However, we have derived general detectors that do not exploit all the properties present in communications signals. For instance, our detectors do not exploit the fact that the transmit pulse shape might be known or that the noise might be temporally and/or spatially uncorrelated.

A. Cyclostationarity vs. Wide-Sense Stationarity

We first compare the performance of the LMPIT and the GLRT with the detectors in [37] (see also [31]) and [28]. These two detectors require selecting which lags and/or harmonics of the cycle frequency to use. This is only possible if the cyclic covariance function is known, which may not be a realistic assumption. For a fair comparison, we decided to use lags 0, 1, 2 and 3 of the cyclic covariance but only one harmonic of the cycle frequency in the detector [28]. However, for the detector [37] we selected the lag that maximizes the cyclic covariance (although this might be unrealistic in practice) because selecting lag 0 would yield poor performance for a QPSK signal with rectangular shaping. Finally, we used a Kaiser window of length 1025 to estimate the cyclic CSM required for the detector [28].

Fig. 3 shows the receiver operating characteristic (ROC) curves for a scenario with global SNR of -16 dB, $L = 3$ antennas, $N = 256$ and $M = 15$. Hence, the total number of samples at each antenna is $NMP = 11520$. As can be seen in the figure, the best performance is provided by the LMPIT, followed by the GLRT. Both LMPIT and GLRT outperform the detectors [28], [37] because they exploit the information at all lags and all harmonics of the cycle frequency. On the contrary, the detector in [37] exploits only the information at one harmonic and one lag. While the detector in [28] utilizes the information at multiple lags and multiple harmonics (although we used only one) they have to be specified *a priori*. In addition to this, the detector in [28] does not take into account the information provided by the cyclic cross-covariance sequences because it is a collaborative detector. The probability of missed detection against the SNR for a fixed false alarm probability $p_{fa} = 10^{-3}$ is depicted in Fig. 4, where similar conclusions can be drawn. One would expect that for some scenarios the performance of the LMPIT compared to the GLRT worsens. Indeed that is the case in Fig. 5. In this experiment we considered a smaller problem in which the hypotheses are not as close (the closeness of the hypotheses depends on the dimension of the covariance matrices, the number of samples, the SNR, ...). Concretely, we selected $L = 2$ sensors, $N = 32$, $P = 2$ (the symbol rate is $R_s = 600$ Kbauds), and $M = 10$. In this scenario, the performance of the GLRT is slightly better than that of the LMPIT.

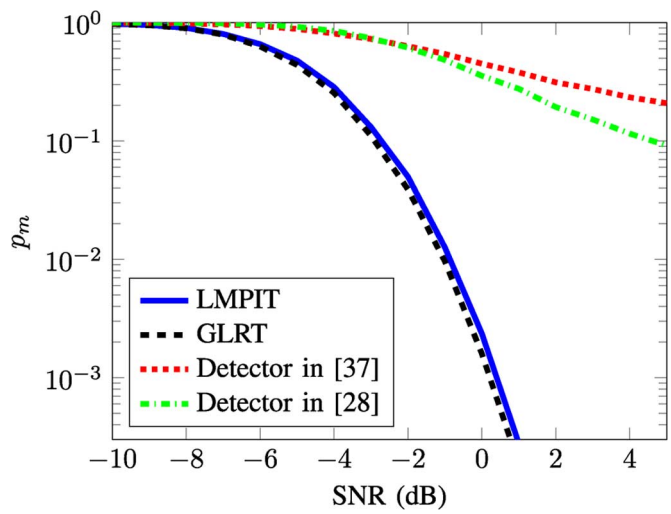

Fig. 5. Probability of missed detection vs. SNR for the test CS vs. WSS in a scenario with $L = 2$, $N = 32$, $P = 2$, and $M = 10$. The probability of false alarm is fixed at $p_{fa} = 10^{-3}$.

B. Null Distribution and Threshold Setting

So far we have not said anything about the threshold, required to fix a probability of false alarm. It is expected that deriving the distributions of the statistics, required for selecting the threshold, is extremely difficult. However, in [59], [60], the

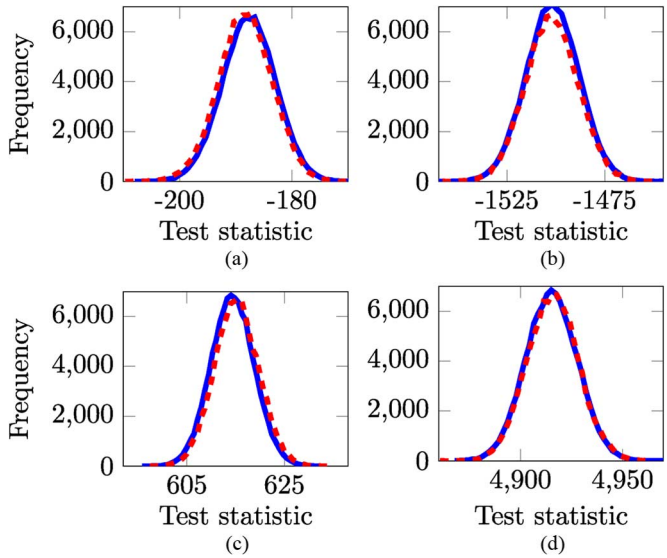

Fig. 6. Comparison between the distributions of the statistics under $\mathcal{H}_0$ for white noise (in blue) and colored noise (in red). (a) GLRT histogram ($N = 32$); (b) GLRT histogram ($N = 256$); (c) LMPIT histogram ($N = 32$); (d) LMPIT histogram ($N = 256$).

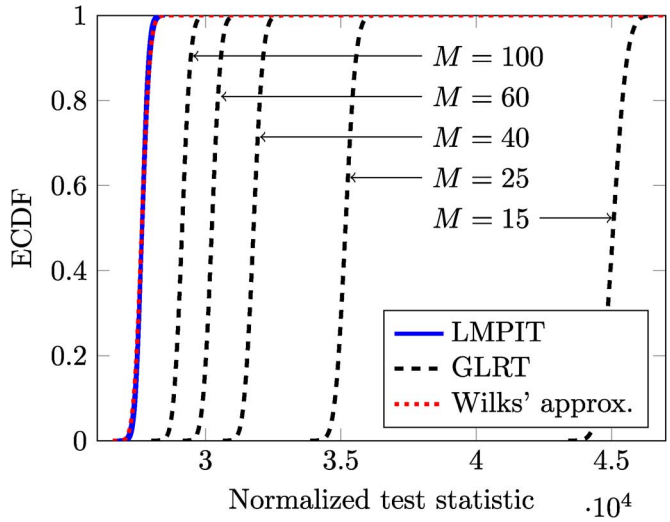

Fig. 7. Empirical cumulative distribution functions (ECDFs) of GLRT and LMPIT statistic for $M = 15, 25, 40, 60$, and 100, and comparison with Wilks' approximation. The LMPIT curve overlays Wilks' approximation.

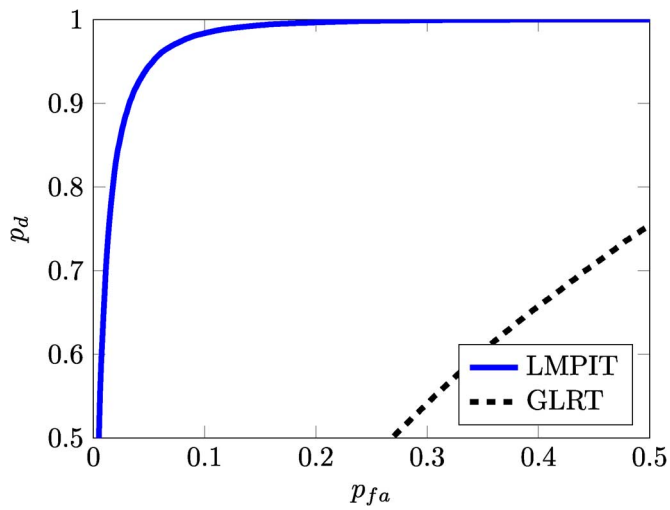

Fig. 8. ROC curves for the test CS vs. NS in a scenario with $L = 2$, $N = 64$, $P = 4$, $M = 400$, and SNR $= -12$ dB.

authors were able to derive a stochastic representation under the null hypothesis, which is applicable to our problem. However, here we will follow a different approach since we want to obtain a closed-form expression for the threshold, which we could not do using the stochastic representation. First, our detectors are invariant to filtering. This means we can obtain the thresholds using numerical simulations for a white process under $\mathcal{H}_0$ and use these thresholds for any arbitrary CSM. But since our LMPIT and GLRT are only *asymptotically* invariant to filtering, this requires some further analysis. We obtained the histograms of the test statistics of our detectors for white noise and colored noise, shown in Fig. 6 for SNR $= -20$ dB. The remaining parameters are the same as in Fig. 3, unless otherwise stated. Figs. 6(a) and 6(b) show the histograms of the GLR for $N = 32$ and $N = 256$, and Figs. 6(c) and 6(d) show the histograms of the LMPIT statistic for $N = 32$ and $N = 256$. The blue lines correspond to white noise and the red lines to colored noise. The differences between red and blue lines are small even for a rather small N, and they further decrease as N increases.

Finally, Wilks' theorem [61] states that the GLR is asymptotically (in M) χ^2-distributed. Because the log-det may be approximated as the Frobenius norm for close hypotheses [44], [62], the LMPIT statistic is also asymptotically χ^2-distributed. So the asymptotic distributions of the GLR and LMPIT statistic are, respectively,

$$-2M \log\det\left(\hat{\mathbf{C}}_L^{LP}\right) \overset{\mathcal{H}_0}{\sim} \chi^2_{L^2NP(P-1)}, \tag{70}$$

$$\left(M\left\|\hat{\mathbf{C}}_L^{LP}\right\|^2 - LNMP\right) \overset{\mathcal{H}_0}{\sim} \chi^2_{L^2NP(P-1)}. \tag{71}$$

These distributions are shown in Fig. 7 for $M = 15, 25, 40, 60$, and 100. These results show that the LMPIT statistic converges much faster to the χ^2 distribution than the GLR. This is an interesting result since Wilks' theorem was derived to compute the asymptotic distribution of the GLRT. These results show that we may also use it for the distribution of the LMPIT, and its convergence is even much faster. To conclude, for large enough M the χ^2 distribution may be used to set the threshold for both the GLRT and the LMPIT.

C. Cyclostationarity vs. Nonstationarity

Finally, we evaluate the performance of the GLRT and the LMPIT for the test $\mathcal{H}_1$ vs. $\mathcal{H}_2$. Fig. 8 shows the ROC curves for these two detectors in an experiment with $L = 2$ antennas, $N = 64$, $M = 400$, and SNR $= -12$ dB. At this SNR, the LMPIT performs much better than the GLRT. It is to be expected, however, that at higher SNRs the GLRT will outperform the LMPIT. As we are not aware of any competing detector, no other comparisons are shown.

VIII. Conclusions

We have presented an asymptotic GLRT and LMPIT for testing whether a multivariate discrete-time process is CS. Most of the state-of-the-art detectors are imaginative but ad-hoc. Our

detectors, on the other hand, are based on established statistical principles. In the time domain, our detectors test the structure of the covariance matrix of the observations. In the frequency domain, the detectors "CS vs. WSS" compare the strength of the CS components with the WSS component. This is also the idea behind many of the state-of-the-art detectors, but the key is to use the right function for this comparison, which optimally fuses the information in the 2D frequency spectrum. Indeed, simulation results have shown that our detectors outperform previously published detectors.

Our hypothesis tests are binary, where the alternative hypothesis is either a WSS or a NS process. We did not consider a multiple hypothesis test (CS, WSS, NS) but the technique proposed in [63] could be directly applied to design a multiple hypothesis GLRT. The main idea behind the technique in [63] is that the sum of the log-GLR for testing CS vs. WSS and the log-GLR for testing CS vs. NS signals is equal to the log-GLR for testing NS vs. WSS signals. Using this relationship it is possible to divide the space spanned by the two GLRs into three regions, where each of these regions corresponds to a one of the hypotheses (CS, WSS, NS). Since this approach is suboptimal, applying it to design a multiple hypothesis LMPIT does not make as much sense since the optimality of the LMPIT would be lost.

Appendix A
Wijsman's Theorem: An Alternative Derivation for the UMPIT

The derivation of the UMPIT usually requires the derivation of the maximal invariant statistic and its distribution under both hypotheses [49]. For many problems this is extremely difficult or even impossible, preventing the derivation of the UMPIT. There is, however, an alternative based on Wijsman's theorem [38], [64], [65]. This theorem states that, under some mild conditions, the ratio of the distributions of the maximal invariant statistic may be obtained as

$$\mathcal{L} = \frac{\int_{\mathcal{G}} p\left(g(\mathbf{x}); \mathcal{H}_1\right) \left|\det(\mathbf{J}_g)\right| dg}{\int_{\mathcal{G}} p\left(g(\mathbf{x}); \mathcal{H}_0\right) \left|\det(\mathbf{J}_g)\right| dg}, \tag{72}$$

where $p(g(\mathbf{x}); \mathcal{H}_i)$ is the probability density function of the transformed observations under the hypothesis $\mathcal{H}_i$, $\mathcal{G}$ is the group of invariant transformations, $\mathbf{J}_g$ denotes the Jacobian of the transformation $g(\cdot) \in \mathcal{G}$ and dg is an invariant group measure, which we take as the usual Lebesgue measure. Even though Wijsman's theorem is quite powerful, it has not received much attention in the signal processing literature, with a few notable exceptions [39], [41], [44], [66]–[70].

The main idea behind Wijsman's theorem was first proposed by Stein [40]. However, the conditions under which (72) is valid were studied much later by Wijsman and other authors in [38], [64], [66], [71]–[73]. For our problem it suffices to consider the simplest conditions. These specify that the group of invariant transformations $\mathcal{G}$ must be a Lie group, a finite group or a composition of both, and the observations must belong to a linear Cartan $\mathcal{G}$-space.[4] Since the set of invertible block-diagonal matrices is a Lie group, the permutation group is a finite group, and the observations belong to a linear Cartan $\mathcal{G}$-space, we may apply Wijsman's theorem to our problem.

[4]A linear Cartan $\mathcal{G}$-space is a nonempty open subset (denoted as $\mathcal{S}$) of the Euclidean space such that, for every $\mathbf{x} \in \mathcal{S}$, there exists a neighborhood $\mathcal{V}$ for which the closure of $\{g(\cdot) \in \mathcal{G} : g(\mathcal{V}) \cap \mathcal{V} \neq \emptyset\}$ is compact.

Appendix B
Proof of Lemma 1

We first simplify the denominator. Ignoring the term $\det(\mathbf{D}_0)$, which does not depend on data or the invariant transformations, the integral in the denominator is given by

$$\int_{\mathbb{D}_{B_0}} \left|\det(\mathbf{G})^{2M}\right| \exp\left[-M\mathrm{tr}\left(\mathbf{D}_0^{-1}\mathbf{P}\mathbf{G}\hat{\mathbf{S}}\mathbf{G}^H\mathbf{P}^T\right)\right] d\mathbf{G}. \tag{73}$$

Taking into account the block-diagonal structure of $\mathbf{D}_0$ and $\mathbf{G}$, with block size B_0, and the fact that the permutation $\mathbf{P}$ keeps such structure, the integral may be rewritten as

$$\int_{\mathbb{D}_{B_0}} \left|\det(\mathbf{G})^{2M}\right| \exp\left[-M\mathrm{tr}\left(\mathbf{D}_0^{-1}\mathbf{P}\mathbf{G}\mathrm{diag}_{B_0}(\hat{\mathbf{S}})\mathbf{G}^H\mathbf{P}^T\right)\right] d\mathbf{G}. \tag{74}$$

Applying now the change of variables $\mathbf{G} \rightarrow \mathbf{G}[\mathrm{diag}_{B_0}(\hat{\mathbf{S}})]^{-1/2}$, the integral becomes

$$\int_{\mathbb{D}_{B_0}} \left|\det(\mathbf{G})^{2M}\right| \exp\left[-M\mathrm{tr}\left(\mathbf{D}_0^{-1}\mathbf{P}\mathbf{G}\mathbf{G}^H\mathbf{P}^T\right)\right] d\mathbf{G}, \tag{75}$$

which does not depend on the observations. Thus, the ratio does not depend on the denominator, which means

$$\mathcal{L} \propto \sum_{\mathbb{P}_\kappa, \mathbb{P}_\mu} \int_{\mathbb{D}_{B_0}} \left|\det(\mathbf{G})^{2M}\right| \times \exp\left[-M\mathrm{tr}\left(\mathbf{D}_1^{-1}\mathbf{P}\mathbf{G}\hat{\mathbf{S}}\mathbf{G}^H\mathbf{P}^T\right)\right] d\mathbf{G}, \tag{76}$$

where we have also removed $\det(\mathbf{D}_1)$. It is possible to substitute $\hat{\mathbf{S}}$ by $\mathrm{diag}_{B_1}(\hat{\mathbf{S}})$ in $\mathcal{L}$ due to the block-diagonal structure of $\mathbf{D}_1$ and $\mathbf{G}$, with block size B_1 in this case. Additionally, the change of variables $\mathbf{G} \rightarrow \mathbf{G}[\mathrm{diag}_{B_0}(\hat{\mathbf{S}})]^{-1/2}$ allows us to write

$$\mathcal{L} \propto \sum_{\mathbb{P}_\kappa, \mathbb{P}_\mu} \int_{\mathbb{D}_{B_0}} \left|\det(\mathbf{G})^{2M}\right| \times \exp\left[-M\mathrm{tr}\left(\mathbf{D}_1^{-1}\mathbf{P}\mathbf{G}\hat{\mathbf{C}}\mathbf{G}^H\mathbf{P}^T\right)\right] d\mathbf{G}, \tag{77}$$

For every permutation we may find a matrix $\mathbf{G} \in \mathbb{D}_{B_0}$, such that the $B_0 \times B_0$ diagonal blocks of $\mathbf{D}_1^{-1}$ are $\mathbf{I}_{B_0}$, which yields

$$\mathcal{L} \propto \sum_{\mathbb{P}_\kappa, \mathbb{P}_\mu} \int_{\mathbb{D}_{B_0}} \left|\det(\mathbf{G})^{2M}\right| \exp\left[-M\mathrm{tr}(\tilde{\mathbf{D}}\mathbf{G}\hat{\mathbf{C}}\mathbf{G}^{\mathbf{H}})\right] d\mathbf{G}. \tag{78}$$

It is clear that for any permutation in $\mathcal{G}$, the matrix $\tilde{\mathbf{D}}$ is block-diagonal, which allows us to simplify the exponent as

$$\mathrm{tr}(\tilde{\mathbf{D}}\mathbf{G}\hat{\mathbf{C}}\mathbf{G}^{\mathbf{H}}) = \sum_{k=1}^{\kappa} \mathrm{tr}\left(\tilde{\mathbf{D}}_k\mathbf{G}_k\hat{\mathbf{C}}_k\mathbf{G}_k^H\right). \tag{79}$$

Finally, since the diagonal blocks of both $\tilde{\mathbf{D}}_k$ and $\hat{\mathbf{C}}_k$ are the identity matrix, the proof follows.

APPENDIX C
PROOF OF THEOREM 7

For close hypotheses (for instance, the CS process is almost WSS) the inverse of the whitened covariance matrix is $\tilde{\mathbf{D}} \approx \mathbf{I}_{\kappa \cdot B_1}$, which implies $\alpha \approx 0$. We may therefore use a second order Taylor's series to approximate $e^{-\alpha}$ to obtain

$$\mathcal{L} \propto \sum_{\mathbb{P}_\kappa, \mathbb{P}_\mu} \int_{\mathbb{D}_{B_0}} \beta(\mathbf{G})(\alpha^2 - 2\alpha) d\mathbf{G}. \tag{80}$$

We now prove that the linear term, given by

$$\sum_{\mathbb{P}_\kappa, \mathbb{P}_\mu} \sum_{k=1}^{\kappa} \sum_{\substack{l,m=1 \\ l \neq m}}^{\mu} \int_{\mathbb{D}_{B_0}} \beta(\mathbf{G}) \mathrm{tr}\left(\tilde{\mathbf{D}}_k^{(lm)} \mathbf{G}_k^{(m)} \hat{\mathbf{C}}_k^{(ml)} \mathbf{G}_k^{(l)H} \right) d\mathbf{G}, \tag{81}$$

must be zero. To do so, let us apply the change of variables $\mathbf{G}_k^{(l)} \rightarrow -\mathbf{G}_k^{(l)}$ for all possible values of k and l. Thus, the integrals become equal to their opposites, which shows that they are indeed zero. Using the same change of variables, it is easy to show that the cross-products in the quadratic term must also be zero, and $\mathcal{L}$ becomes

$$\mathcal{L} \propto \sum_{\mathbb{P}_\kappa, \mathbb{P}_\mu} \sum_{k=1}^{\kappa} \sum_{\substack{l,m=1 \\ l \neq m}}^{\mu} \int_{\mathbb{D}_{B_0}} \beta(\mathbf{G}) \times \mathrm{tr}^2 \left(\tilde{\mathbf{D}}_k^{(lm)} \mathbf{G}_k^{(m)} \hat{\mathbf{C}}_k^{(ml)} \mathbf{G}_k^{(l)H} \right) d\mathbf{G}. \tag{82}$$

By introducing another change of variables, which involves the matrices of left and singular vectors of $\tilde{\mathbf{D}}_k^{(lm)}$ and $\hat{\mathbf{C}}_k^{(ml)}$, the ratio of the distributions is only a function of the singular values, that is,

$$\mathcal{L} \propto \sum_{\mathbb{P}_\kappa, \mathbb{P}_\mu} \sum_{k=1}^{\kappa} \sum_{\substack{l,m=1 \\ l \neq m}}^{\mu} \int_{\mathbb{D}_{B_0}} \beta(\mathbf{G}) \times \left(\sum_{t,s=1}^{B_0} \left[\tilde{\mathbf{\Lambda}}_k^{(lm)} \right]_{t,t} \left[\hat{\Xi}_k^{(lm)} \right]_{s,s} \left[\mathbf{G}_k^{(m)} \right]_{t,s} \left[\mathbf{G}_k^{(l)} \right]_{t,s}^* \right)^2 d\mathbf{G}, \tag{83}$$

where $\tilde{\mathbf{\Lambda}}_k^{(lm)}$ and $\hat{\Xi}_k^{(lm)}$ are diagonal matrices that contain the singular values of $\tilde{\mathbf{D}}_k^{(lm)}$ and $\hat{\mathbf{C}}_k^{(ml)}$, respectively. The change of variables $[\mathbf{G}_k^{(m)}]_{t,s} \rightarrow -[\mathbf{G}_k^{(m)}]_{t,s}$ allows us to get rid of the cross-terms in the square, which yields

$$\mathcal{L} \propto \sum_{\mathbb{P}_\kappa, \mathbb{P}_\mu} \sum_{k=1}^{\kappa} \sum_{\substack{l,m=1 \\ l \neq m}}^{\mu} \sum_{t,s=1}^{B_0} \left[\tilde{\mathbf{\Lambda}}_k^{(lm)} \right]_{t,t}^2 \left[\hat{\Xi}_k^{(lm)} \right]_{s,s}^2 \Delta, \tag{84}$$

where

$$\Delta = \int_{\mathbb{D}_{B_0}} \beta(\mathbf{G}) \mathrm{Re}\left[\left(\left[\mathbf{G}_k^{(m)} \right]_{t,s} \left[\mathbf{G}_k^{(l)} \right]_{t,s}^* \right)^2 \right] d\mathbf{G}. \tag{85}$$

For the considered values of k, l, m, s and t, the integral Δ takes the same value regardless of the indices, and the ratio simplifies to

$$\mathcal{L} \propto \sum_{\mathbb{P}_\kappa, \mathbb{P}_\mu} \sum_{k=1}^{\kappa} \sum_{\substack{l,m=1 \\ l \neq m}}^{\mu} \sum_{t=1}^{B_0} \left[\tilde{\mathbf{\Lambda}}_k^{(lm)} \right]_{t,t}^2 \sum_{s=1}^{B_0} \left[\hat{\Xi}_k^{(lm)} \right]_{s,s}^2. \tag{86}$$

Noting that the sum of the squared singular values is the squared Frobenius norm, the ratio therefore becomes

$$\mathcal{L} \propto \sum_{k=1}^{\kappa} \sum_{\substack{l,m=1 \\ l>m}}^{\mu} \left\| \hat{\mathbf{C}}_k^{(ml)} \right\|^2 \left(\sum_{\mathbb{P}_\kappa, \mathbb{P}_\mu} \left\| \tilde{\mathbf{D}}_k^{(lm)} \right\|^2 \right). \tag{87}$$

The sum over all possible permutations of the blocks $\tilde{\mathbf{D}}_k^{(lm)}$ establishes that the term within parentheses is independent of the indices k, l and m. Moreover, it can be shown that this sum is given by

$$\sum_{\mathbb{P}_\kappa, \mathbb{P}_\mu} \left\| \tilde{\mathbf{D}}_k^{(lm)} \right\|^2 \propto \|\tilde{\mathbf{D}}\|^2, \tag{88}$$

which yields

$$\mathcal{L} \propto \sum_{k=1}^{\kappa} \sum_{\substack{l,m=1 \\ l>m}}^{\mu} \left\| \hat{\mathbf{C}}_k^{(ml)} \right\|^2. \tag{89}$$

Finally, taking into account that $\|\hat{\mathbf{C}}_k^{(ml)}\|^2 = \|\hat{\mathbf{C}}_k^{(lm)}\|^2$ and $\|\hat{\mathbf{C}}_k^{(mm)}\|^2 = B_0$, the proof follows.

REFERENCES

[1] W. A. Gardner, *Introduction to Random Processes with Applications to Signal and Systems*. New York, NY, USA: Macmillan, 1985.

[2] H. L. Hurd, "An investigation of periodically correlated stochastic processes," Ph.D. dissertation, Duke Univ., Durham, NC, USA, 1969.

[3] W. A. Gardner, W. Brown, and C.-K. Chen, "Spectral correlation of modulated signals: Part II—Digital modulation," *IEEE Trans. Commun.*, vol. 35, no. 6, pp. 595–601, Jun. 1987.

[4] P. Bloomfield, H. L. Hurd, and R. B. Lund, "Periodic correlation in stratospheric ozone data," *J. Time Ser. Anal.* vol. 15, no. 2, pp. 127–150, 1994 [Online]. Available: http://dx.doi.org/10.1111/j.1467-9892.1994.tb00181.x

[5] R. J. Dargaville, S. C. Doney, and I. Y. Fung, "Inter-annual variability in the interhemispheric atmospheric CO2 gradient: Contributions from transport and the seasonal rectifier," *Tellus B* vol. 55, no. 2, pp. 711–722, 2003 [Online]. Available: http://dx.doi.org/10.1034/j.1600-0889.2003.00038.x

[6] S. Ghosh, P. Sen, and U. De, "Identification of significant parameters for the prediction of pre-monsoon thunderstorms at calcutta, india," *Int. J. Climatol.* vol. 19, no. 6, pp. 673–681, 1999 [Online]. Available: http://dx.doi.org/10.1002/(SICI)1097-0088(199905)19:6<673::AID-JOC384>3.0.CO;2-O

[7] D. Bukofzer, "Optimum and suboptimum detector performance for signals in cyclostationary noise," *IEEE J. Ocean. Eng.*, vol. 12, no. 1, pp. 97–115, Jan. 1987.

[8] A. V. Dandawate and G. B. Giannakis, "Extraction of acoustic signals using cyclostationarity," in *Underwater Signal Processing Workshop*, Providence, RI, USA, Oct. 1993.

[9] A. Kacimov, Y. Obnosov, and N. Yakimov, "Groundwater flow in a medium with a parquet-type conductivity distribution," *J. Hydrol.* vol. 226, no. 3–4, pp. 242–249, 1999 [Online]. Available: http://www.sciencedirect.com/science/article/pii/S0022169499001511

[10] H. L. Hurd and C. H. Jones, "Dynamical systems with cyclostationary orbits," in *Proc. Amer. Inst. Phys. Conf. Ser.*, May 1994, vol. 296, pp. 246–259.

[11] E. Broszkiewicz-Suwaj, A. Makagon, R. Weron, and A. Wylomańska, "On detecting and modeling periodic correlation in financial data," *Phys. A: Statist. Mechan. Appl.*, vol. 336, pp. 196–205, May 2004.

[12] P. Franses, *Periodicity and Stochastic Trends in Economic Time Series*, ser. Advanced Texts in Econometrics. Oxford, U.K.: Oxford Univ. Press, 1996.

[13] E. Ghylsels and D. R. Osborn, *The Econometric Analysis of Seasonal Time Series*. New York, NY, USA: Cambridge Univ. Press, 2001.

[14] E. Serpedin, F. Panduru, I. Sar, and G. B. Giannakis, "Bibliography on cyclostationarity," *Signal Process.*, vol. 85, no. 12, pp. 2233–2303, 2005.

[15] W. A. Gardner, A. Napolitano, and L. Paura, "Cyclostationarity: Half a century of research," *Signal Process.*, vol. 86, no. 4, pp. 639–697, 2006.

[16] D. Cabric, "Addressing the feasibility of cognitive radios," *IEEE Signal Process. Mag.*, vol. 25, no. 6, pp. 85–93, Nov. 2008.

[17] K.-C. Chen and R. Prasad, *Cognitive Radio Networks*. New York, NY, USA: Wiley, 2009.

[18] J. Mitola and G. Q. Maguire, Jr., "Cognitive radio: Making software radios more personal," *IEEE Pers. Commun.*, vol. 6, pp. 13–18, Aug. 1999.

[19] E. Axell, G. Leus, E. Larsson, and H. Poor, "Spectrum sensing for cognitive radio: State-of-the-art and recent advances," *IEEE Signal Process. Mag.*, vol. 29, no. 3, pp. 101–116, May 2012.

[20] E. Broszkiewicz-Suwaj, Methods for determining the presence of periodic correlation based on the bootstrap methodology Wrocław Univ. Technol., Tech. Rep. Res. Rep. HSC/03/2, 2003.

[21] H. L. Hurd and N. L. Gerr, "Graphical methods for determining the presence of periodic correlation," *J. Time Ser. Anal.*, vol. 12, no. 4, pp. 337–350, 1991.

[22] A. V. Dandawaté and G. B. Giannakis, "Statistical tests for presence of cyclostationarity," *IEEE Trans. Signal Process.*, vol. 42, no. 9, pp. 2355–2369, Sep. 1994.

[23] S. Enserink and D. Cochran, "On detection of cyclostationary signals," in *Proc. IEEE Int. Conf. Acoust., Speech Signal Process. (ICASSP)*, Detroit, USA, May 1995, pp. 2004–2007.

[24] E. Axell and E. G. Larsson, "Multiantenna spectrum sensing of a second-order cyclostationary signal," in *Proc. IEEE Int. Work. Comp. Adv. in Multi-Sens. Adapt. Process.*, Dec. 2011, pp. 329–332.

[25] X. Chen, W. Xu, Z. He, and X. Tao, "Spectral correlation-based multi-antenna spectrum sensing technique," in *Proc. IEEE Wireless Comm. Netw. Conf.*, Mar. 2008, pp. 735–740.

[26] G. Huang and J. K. Tugnait, "On cyclostationarity based spectrum sensing under uncertain Gaussian noise," *IEEE Trans. Signal Process.*, vol. 61, no. 8, pp. 2042–2054, Apr. 2013.

[27] J. Lundén, S. Kassam, and V. Koivunen, "Robust nonparametric cyclic correlation-based spectrum sensing for cognitive radios," *IEEE Trans. Signal Process.*, vol. 58, no. 6, pp. 38–52, Jun. 2010.

[28] J. Lundén, V. Koivunen, A. Huttunen, and H. V. Poor, "Collaborative cyclostationary spectrum sensing for cognitive radio systems," *IEEE Trans. Signal Process.*, vol. 57, no. 11, pp. 4182–4195, Nov. 2009.

[29] E. Rebeiz, P. Urriza, and D. Cabric, "Optimizing wideband cyclostationary spectrum sensing under receiver impairments," *IEEE Trans. Signal Process.*, vol. 61, no. 15, pp. 3931–3943, Aug. 2013.

[30] J. Riba, J. Font-Segura, J. Villares, and G. Vazquez, "Frequency-domain GLR detection of a second-order cyclostationary signal over fading channels," *IEEE Trans. Signal Process.*, vol. 62, no. 8, pp. 1899–1912, Apr. 2014.

[31] P. Urriza, E. Rebeiz, and D. Cabric, "Multiple antenna cyclostationary spectrum sensing based on the cyclic correlation significance test," *IEEE J. Sel. Areas Commun.*, vol. 31, no. 11, pp. 2185–2195, Nov. 2013.

[32] M. Loève, *Probability Theory II*, 4th ed. New York, NY, USA: Springer-Verlag, 1978.

[33] E. D. Gladyshev, "Periodically correlated random sequences," *Soviet Math. Dokl.*, vol. 2, pp. 385–388, 1961.

[34] J.-C. Shen and E. Alsusa, "Joint cycle frequencies and lags utilization in cyclostationary feature spectrum sensing," *IEEE Trans. Signal Process.*, vol. 61, no. 21, pp. 5337–5346, Nov. 2013.

[35] A. V. Vecchia and R. Ballerini, "Testing for periodic autocorrelations in seasonal time series data," *Biometrika*, vol. 78, no. 1, pp. 53–63, 1991.

[36] W. Gardner, "Exploitation of spectral redundancy in cyclostationary signals," *IEEE Signal Process. Mag.*, vol. 8, no. 2, pp. 14–36, Apr. 1991.

[37] S. Schell and W. Gardner, "Detection of the number of cyclostationary signals in unknown interference and noise," in *Proc. Asilomar Conf. Signals, Syst. Comput.*, Nov. 1990, vol. 1, p. 473.

[38] R. A. Wijsman, "Cross-sections of orbits and their application to densities of maximal invariants," in *Proc. 5th Berkeley Symp. Math. Stat. Prob.*, 1967, vol. 1, pp. 389–400.

[39] J. R. Gabriel and S. M. Kay, "Use of Wijsman's theorem for the ratio of maximal invariant densities in signal detection applications," in *Proc. Asilomar Conf. Signals, Syst. Comput.*, Nov. 2002, vol. 1, pp. 756–762.

[40] C. Stein, Some Problems in Multivariate Analysis, part 1 Stanford Univ. Dept. Statist., Tech. Rep., 1956.

[41] A. A. D'Amico, "IR-UWB transmitted-reference systems with partial channel knowledge: A receiver design based on the statistical invariance principle," *IEEE Trans. Signal Process.*, vol. 59, no. 4, pp. 1435–1448, Apr. 2011.

[42] D. Cochran, H. Gish, and D. Sinno, "A geometric approach to multiple-channel signal detection," *IEEE Trans. Signal Process.*, vol. 43, no. 9, pp. 2049–2057, Sep. 1995.

[43] D. Ramírez, J. Vía, I. Santamaría, and L. L. Scharf, "Detection of spatially correlated Gaussian time series," *IEEE Trans. Signal Process.*, vol. 58, no. 10, Oct. 2010.

[44] D. Ramírez, J. Vía, I. Santamaría, and L. L. Scharf, "Locally most powerful invariant tests for correlation and sphericity of Gaussian vectors," *IEEE Trans. Inf. Theory*, vol. 59, no. 4, pp. 2128–2141, Apr. 2013.

[45] P. J. Schreier and L. L. Scharf, *Statistical Signal Processing of Complex-Valued Data*. Cambridge, U.K.: Cambridge Univ. Press, 2010.

[46] D. Ramírez, G. Vázquez-Vilar, R. López-Valcarce, J. Vía, and I. Santamaría, "Detection of rank- P signals in cognitive radio networks with uncalibrated multiple antennas," *IEEE Trans. Signal Process.*, vol. 59, no. 8, pp. 3764–3774, Aug. 2011.

[47] D. Ramírez, L. L. Scharf, J. Vía, I. Santamaría, and P. J. Schreier, "An asymptotic GLRT for the detection of cyclostationary signals," in *Proc. IEEE Int. Conf. Acoust., Speech Signal Process.*, Florence, Italy, May 2014.

[48] K. V. Mardia, J. T. Kent, and J. M. Bibby, *Multivariate Analysis*. New York: Academic, 1979.

[49] L. L. Scharf, *Statistical Signal Processing: Detection, Estimation, Time Series Analysis*. Norwood, MA, USA: Addison-Wesley, 1991.

[50] R. M. Gray, "Toeplitz and circulant matrices: A review," *Found. Trends Commun. Inf. Theory*, vol. 2, no. 3, pp. 155–219, 2006.

[51] J. Gutiérrez-Gutiérrez and P. M. Crespo, "Asymptotically equivalent sequences of matrices and Hermitian block Toeplitz matrices with continuous symbols: Applications to MIMO systems," *IEEE Trans. Inf. Theory*, vol. 54, no. 12, pp. 5671–5680, Dec. 2008.

[52] J. R. Magnus and H. Neudecker, "The commutation matrix: Some properties and applications," *Ann. Statist.*, vol. 7, no. 2, pp. 381–394, Mar. 1979.

[53] J. W. Cooley and J. W. Tukey, "An algorithm for the machine calculation of complex Fourier series," *Math. Comput.*, vol. 19, no. 90, pp. 297–301, 1965.

[54] J. R. Magnus and H. Neudecker, *Matrix Differential Calculus with Applications in Statistics and Econometrics*. New York, NY, USA: Wiley, 1999.

[55] M. Puschel and J. M. F. Moura, "Algebraic signal processing theory: Cooley-Tukey type algorithms for DCTs and DSTs," *IEEE Trans. Signal Process.*, vol. 56, no. 4, pp. 1502–1521, Apr. 2008.

[56] L. Izzo and A. Napolitano, "The higher order theory of generalized almost-cyclostationary time series," *IEEE Trans. Signal Process.*, vol. 46, no. 11, pp. 2975–2989, Nov. 1998.

[57] A. Napolitano, "Generalizations of cyclostationarity: A new paradigm for signal processing for mobile communications, Radar, Sonar," *IEEE Signal Process. Mag.*, vol. 30, no. 6, pp. 53–63, Nov. 2013.

[58] A. Napolitano, *Generalizations of Cyclostationary Signal Processing: Spectral Analysis and Applications*, ser. Wiley-IEEE. Hoboken, NJ, USA: Wiley, 2012.

[59] N. Klausner, M. Azimi-Sadjadi, L. L. Scharf, and D. Cochran, "Space-time coherence and its exact null distribution," in *Proc. IEEE Int. Conf. on Acoust., Speech Signal Process.*, Vancouver, Canada, May 2013.

[60] N. Klausner, M. Azimi-Sadjadi, and L. L. Scharf, "Detection of spatially correlated time series from a network of sensor arrays," *IEEE Trans. Signal Process.*, vol. 62, no. 6, pp. 1396–1407, Mar. 2014.

[61] S. M. Kay, *Fundamentals of Statistical Signal Processing: Detection Theory*. Englewood Cliffs, NJ, USA: Prentice-Hall, 1998, vol. II.

[62] A. Leshem and A.-J. Van der Veen, "Multichannel detection of Gaussian signals with uncalibrated receivers," *IEEE Signal Process. Lett.*, vol. 8, no. 4, pp. 120–122, Apr. 2001.

[63] J. Vía, D. P. Palomar, and L. Vielva, "Generalized likelihood ratios for testing the properness of quaternion Gaussian vectors," *IEEE Trans. Signal Process.*, vol. 59, no. 4, pp. 1356–1370, Apr. 2011.

[64] M. L. Eaton, *Group Invariance Applications in Statistics*. New York, NY, USA: Inst. Math. Stat., 1989.

[65] N. C. Giri, *Multivariate statistical analysis*, ser. Statistics, textbooks and monographs. New York, NY, USA: Marcel Dekker, 2004.

[66] J. R. Gabriel and S. M. Kay, "On the relationship between the GLRT and UMPI tests for the detection of signals with unknown parameters," *IEEE Trans. Signal Process.*, vol. 53, no. 11, pp. 4194–4203, Nov. 2005.

[67] R. E. Schwartz, "Minimax CFAR detection in additive Gaussian noise of unknown covariance," *IEEE Trans. Inf. Theory*, vol. 15, no. 6, pp. 722–725, Nov. 1969.

[68] J. Vía and L. Vielva, "Locally most powerful invariant tests for the properness of quaternion Gaussian vectors," *IEEE Trans. Signal Process.*, vol. 60, no. 3, Mar. 2012.

[69] D. Ramírez, J. Iscar, J. Vía, I. Santamaría, and L. L. Scharf, "The locally most powerful invariant test for detecting a rank- p Gaussian signal in white noise," in *Proc. IEEE Sens. Array Multichannel Signal Process. Work.*, Hoboken, NJ, USA, Jun. 2012.

[70] D. Ramírez, J. Vía, and I. Santamaría, "The locally most powerful test for multiantenna spectrum sensing with uncalibrated receivers," in *Proc. IEEE Int. Conf. Acoust., Speech Signal Process.*, Kyoto, Japan, Mar. 2012.

[71] R. A. Wijsman, *Invariant Measures On Groups And Their Use In Statistics*. New York, NY, USA: Inst. Math. Stat., 1990.
[72] R. A. Wijsman, "Proper action in steps, with application to density ratios of maximal invariants," *Ann. Statist.*, vol. 13, no. 1, pp. 395–402, 1985.
[73] R. A. Wijsman, "Correction: Proper action in steps, with application to density ratios of maximal invariants," *Ann. Statist.*, vol. 21, no. 4, pp. 2168–2169, Dec. 1993.

David Ramírez (S'07–M'12) received the Telecommunication Engineer degree and the Ph.D. degree in Electrical Engineering from the University of Cantabria, Spain, in 2006 and 2011, respectively.

From 2006 to 2011, he was with the Communications Engineering Department, University of Cantabria, Spain. In 2011, he was a Research Associate with the University of Paderborn, Germany, where he is currently an Assistant Professor (Akademischer Rat). He has been a Visiting Researcher at the University of Newcastle, Australia. His current research interests include signal processing for wireless communications, MIMO systems, and statistical signal processing.

Dr. Ramírez has been involved in several national and international research projects on these topics. He was the recipient of the 2012 IEEE Signal Processing Society Young Author Best Paper Award.

Peter J. Schreier (S'03–M'04–SM'09) was born in Munich, Germany, in 1975. He received a Master of Science from the University of Notre Dame, IN, USA, in 1999, and the Ph.D. degree from the University of Colorado at Boulder, USA, in 2003, both in electrical engineering.

In the fall semester of 1998, he was a visiting research student with the Coding Group at the University of Hawaii at Manoa, USA. In the spring semester of 2004, he was a Postdoctoral Research Associate, and in the spring semester of 2008, a Visiting Associate Professor with the Department of Electrical and Computer Engineering at Colorado State University, Ft. Collins, USA. From 2004 until 2011, he was with the School of Electrical Engineering and Computer Science at the University of Newcastle, Australia, first as Lecturer, then Senior Lecturer, and finally Associate Professor. Since 2011, he has been Professor and Head of the Signal and System Theory Group in the Department of Electrical Engineering and Information Technology at Universität Paderborn, Germany.

Dr. Schreier has received fellowships from the State of Bavaria, the Studienstiftung des deutschen Volkes (German National Academic Foundation), and the Deutsche Forschungsgemeinschaft (German Research Foundation). In 2011, he received the Award for "German scientists returning from abroad" from the Alfried Krupp von Bohlen und Halbach foundation. From 2008 until 2012, he was an Associate Editor of the IEEE TRANSACTIONS ON SIGNAL PROCESSING, and from 2010 to 2014 he served as a Senior Area Editor for the same TRANSACTIONS.

Javier Vía (M'08–SM'12) received the Degree in telecommunication engineering and the Ph.D. degree in electrical engineering from the University of Cantabria, Cantabria, Spain, in 2002 and 2007, respectively.

He joined the Department of Communications Engineering, University of Cantabria, in 2002, where he is currently an Associate Professor. He has spent visiting periods at the Smart Antennas Research Group, Stanford University, Stanford, CA, USA, and the Department of Electronics and Computer Engineering, Hong Kong University of Science and Technology, Hong Kong. He has actively participated in several European and Spanish research projects. His current research interests include blind channel estimation and equalization in wireless communication systems, multivariate statistical analysis, quaternion signal processing, and kernel methods.

Ignacio Santamaría (M'96–SM'05) received the Telecommunication Engineer degree and the Ph.D. degree in electrical engineering from the Universidad Politcnica de Madrid (UPM), Spain, in 1991 and 1995, respectively.

In 1992, he joined the Department of Communications Engineering, University of Cantabria, Spain, where he is currently Full Professor. He has coauthored more than 150 publications in refereed journals and international conference papers and holds two patents. His current research interests include signal processing algorithms and information-theoretic aspects of multiuser multiantenna wireless communication systems, multivariate statistical techniques and machine learning theories. He has been involved in numerous national and international research projects on these topics. He has been a visiting researcher at the Computational NeuroEngineering Laboratory (University of Florida), and at the Wireless Networking and Communications Group (The University of Texas at Austin).

Dr. Santamara was a Technical Co-Chair of the 2nd International ICST Conference on Mobile Lightweight Wireless Systems (MOBILIGHT 2010), Special Sessions Co-Chair of the 2011 European Signal Processing Conference (EUSIPCO 2011), and General Co-Chair of the 2012 IEEE Workshop on Machine Learning for Signal Processing (MLSP 2012). From 2009 to 2014, he was a member of the IEEE Machine Learning for Signal Processing Technical Committee. Currently, he serves as Associate Editor and Senior Area Editor of the IEEE TRANSACTIONS ON SIGNAL PROCESSING. He was a corecipient of the 2008 EEEfCOM Innovation Award, as well as coauthor of a paper that received the 2012 IEEE Signal Processing Society Young Author Best Paper Award.

Louis L. Scharf (S'67–M'69–SM'77–F'86–LF'07) received the Ph.D. degree from the University of Washington, Seattle, USA.

From 1971 to 1982, he served as Professor of Electrical Engineering and Statistics with Colorado State University (CSU), Ft. Collins, USA. From 1982 to 1985, he was Professor and Chairman of Electrical and Computer Engineering, University of Rhode Island, Kingston. From 1985 to 2000, he was Professor of Electrical and Computer Engineering, University of Colorado, Boulder, USA. In January 2001, he rejoined CSU as Professor of Electrical and Computer Engineering and Statistics. He is currently a Research Professor of Mathematics at CSU. He has held several visiting positions here and abroad, including the Ecole Superieure d'electricité, Gif-sur-Yvette, France; Ecole Nationale Superieure des Télécommunications, Paris, France; EURECOM, Nice, France; the University of La Plata, La Plata, Argentina; Duke University, Durham, NC, USA; the University of Wisconsin, Madison, USA; and the University of Tromsø, Tromsø, Norway. His interests are in statistical signal processing, as it applies to adaptive radar, sonar, and wireless communication.

Prof. Scharf was Technical Program Chair for the 1980 IEEE International Conference on Acoustics, Speech, and Signal Processing (ICASSP), Denver, CO, USA; Tutorials Chair for ICASSP 2001, Salt Lake City, UT, USA; and Technical Program Chair for the Asilomar Conference on Signals, Systems, and Computers 2002. He is past-Chair of the Fellow Committee for the IEEE Signal Processing Society. He has received numerous awards for his research contributions to statistical signal processing, including a College Research Award, an IEEE Distinguished Lectureship, an IEEE Third Millennium Medal, and the Technical Achievement and Society Awards from the IEEE Signal Processing Society.